Journal of Molecular Spectroscopy **208,** 121–135 (2001)
doi:10.1006/jmsp.2001.8367, available online at http://www.idealibrary.com on IDEAL®

The Energy Levels of the $\nu_5/2\nu_9$ Dyad of HNO_3 from Millimeter and Submillimeter Rotational Spectroscopy

Douglas T. Petkie,* Thomas M. Goyette,† Paul Helminger,‡ Herb M. Pickett,§ and Frank C. De Lucia¶

*Department of Physics, Ohio Northern University, Ada, Ohio 45810; †Department of Physics, University of Massachusetts at Lowell, Lowell, Massachusetts 01854; ‡Department of Physics, University of South Alabama, Mobile, Alabama 36688; §Jet Propulsion Laboratory, California Institute of Technology, Pasadena, California 91109; and ¶Department of Physics, The Ohio State University, Columbus, Ohio 43210

Received March 22, 2001

In this paper we show that the rotational structure of the $\nu_5/2\nu_9$ infrared band near 11 μm can be synthesized to high accuracy from pure rotational measurements in the millimeter- and submillimeter-wave region. The analysis uses an internal axis system Hamiltonian that accounts for the rotational dependence of the torsional splitting in $2\nu_9$, the induced torsional splitting in ν_5, and all of the infrared line positions, including those in the regions of strongest mixing and of highest excitation. This model also predicts the strength of the $2\nu_9$ infrared band due to the strong Fermi mixing with ν_5. The analysis is based on the 2317 millimeter/submillimeter lines and uses the well-documented SPFIT routines of JPL.

Key Words: nitric acid; ν_5; $2\nu_9$; HNO_3; millimeter; infrared; spectra; spectroscopy.

I. INTRODUCTION

Nitric acid (HNO_3) has been extensively studied in both the microwave and infrared spectral regions because it is both a fundamental chemical species and an important constituent of the upper atmosphere. This is especially true for the ν_5 (NO_2 in plane bend) and $2\nu_9$ (OH torsion) bands because their strong spectral features occur in the region around 900 cm^{-1}, a favorable region for atmospheric remote sensing. Because a strong Fermi resonance couples these bands into an interacting dyad, the development of their analyses has become intertwined.

The spectrum in this region was first observed at high resolution by Brockman *et al*. (*1*), who measured, but did not assign, a portion of the ν_5 spectrum. Subsequently, Maki and Wells (*2*) measured and assigned transitions in ν_5 and found it was necessary to consider a Fermi resonance with the nearby $2\nu_9$ band. Giesen *et al*. (*3*) were able to resolve the torsional splittings ($\sim$0.002 cm^{-1}/60 MHz) in a diode laser spectrum of about 25 lines of $2\nu_9$. More recently, Maki and Wells (*4*) extended their earlier work to include over 1400 infrared lines in both ν_5 and $2\nu_9$ (as well as 72 unpublished millimeter and submillimeter (mm/submm) ν_5 lines from our laboratory) and published a more detailed analysis of the effect of the Fermi resonance. They, too, observed a small splitting in many of the $2\nu_9$ transitions in their diode laser spectrum. Perrin *et al*. (*5*) also have analyzed this region using as an experimental basis a high-resolution Fourier transform spectrum. Although these data did not resolve the $2\nu_9$ doublets, they did provide for a detailed analysis of the perturbations between the two states.

A number of years ago Crownover *et al*. (*6*) reported in a mm/submm study of the pure rotational spectra of the excited vibrational states the observation of a small ($\sim$2 MHz) torsional splitting in the ν_9 state. More recently, Goyette *et al*. (*7*) observed splittings in the $2\nu_9$($\sim$50 MHz) and, perhaps surprisingly, in ν_5($\sim$35 MHz) as well. Because both of these observed splittings have their physical origin in the torsional motion of the ν_9 vibrational mode, it was possible to use the measured ratio of these splittings to calculate *directly* the mixing of the two "pure" vibrational states. This calculation quantified the value of F_0 at 8.53 cm^{-1} and *predicts* the intensity ratio of the two infrared bands to be 1.43, in good agreement with the observed value of 1.4.

Coudert and Perrin (*8*) then combined the mm/submm observations of the splittings of Ref. (*7*) with their FTIR data set in the context of an IAM Hamiltonian. In this work they determined separate torsional parameters for each of the vibrational states.

More recently (*9*) we reported 860 mm/submm transitions in the symmetric-top limit (i.e., those lines not split by asymmetry) of the $\nu_5/2\nu_9$ dyad. All of these data were analyzed to within experimental accuracy ($\sim$0.1 MHz/3×10^{-6} cm^{-1}) by means of a Hamiltonian which included (1) a set of rotation/distortion constants for each of the torsional states of $2\nu_9$ and a single set for ν_5, and (2) Fermi interaction terms which couple ν_5 and $2\nu_9$. In this model no adjustable parameters were provided for the observed splittings in ν_5, which are effectively predicted by the model from the physically real splittings in $2\nu_9$ and the vibrational interaction terms.

In this paper we present a complete analysis of the $\nu_5/2\nu_9$ dyad using an IAS Hamiltonian that accurately models the rotational

Supplementary data for this article are available on IDEAL (http://www.idealibrary.com) and as part of the Ohio State University Molecular Spectroscopy Archives (http://msa.lib.ohio-state.edu/jmsa_hp.htm).

0022-2852/01 $35.00

dependence of the torsional splitting and the strong Fermi and Coriolis resonances. We compare the results with energy levels derived previously (*5*) from infrared measurements and a model of the mm/submm rotational levels in the ground vibrational state. We will show that the mm/submm analysis accurately predicts the entire rotational manifold of the infrared band. We will also argue that this case is particularly stringent and that this method should be generally applicable.

II. EXPERIMENTAL

Of the 2317 transitions used in this analysis, 860 have been reported previously (*9*). Of the remaining 1457, those above 178 GHz were measured in a FASSST spectrometer with video detection and optical calibration (*10, 11*). Lines between 118 and 178 GHz were measured in a system that used a KVARTZ synthesizer in a conventional FM source modulation mode. For the aforementioned lines, a glass cell of ~ 5 m length and 10 cm diameter was used and the radiation detected with a liquid He-cooled InSb hot electron bolometer. Lines below 118 GHz were either assigned from previous measurements or measured at the Jet Propulsion Laboratory with a phase-locked klystron system, a diode detector, and a 1-m-long double-pass absorption cell, as described in Ref. (*12*). In all cases, the cell pressure was maintained near 10 mTorr to ensure the measured lines had Doppler limited widths. We estimate the accuracy of all the data to be $\sim$100 kHz or better.

III. HAMILTONIAN MODEL AND ANALYSIS

Several approaches have been used to treat the $\nu_5/2\nu_9$ dyad. The most important features are the perturbations that mix the vibrational states and the torsional motion associated with $2\nu_9$. In $2\nu_9$ the large amplitude torsional motion splits the energy levels into two sublevels, half of which are not populated. This leads to two torsional states that share one set of rotational labels, half in each torsional state. For $2\nu_9$ any energy level with $K_a =$ even (symmetric torsional wavefunction) will be shifted down and any level with $K_a =$ odd (antisymmetric torsional wavefunction) will be shifted up (*8*).

We have previously shown that as the Fermi interaction term F_0 between $2\nu_9$ and ν_5 becomes comparable to the vibrational energy splitting ΔE, the mixing of the two states causes the torsional splitting of $2\nu_9$ to be induced onto ν_5 and the values of the *observed* splittings $\delta_{2\nu 9}$ and $\delta_{\nu 5}$ to become nearly equal (*7*). Consequently, in our analysis of the symmetric-top-like states, we have used this mixing to induce from the base torsional states $2\nu_9$ the torsional splittings observed in ν_5 (*9*). An interesting feature of this approach is that by using the observed splitting in each of the bands it is possible to separate the highly correlated Fermi mixing term F_0 and vibrational energy ΔE and determine the mixing coefficients for the combined wavefunction. These mixing coefficients then *predict* the observed infrared intensity of $2\nu_9$, which is primarily "borrowed" from ν_5 (*9*). Alternatively, Coudert and Perrin have shown that the splittings can be analyzed in the context of an IAM approach with a different set of torsional parameters for $2\nu_9$ and ν_5 (*8*).

In our earlier analysis of the symmetric-top-like transitions, we used SPFIT (*13*) in the induced splitting mode described above. Predictions from this analysis served as a starting point for assigning transitions with asymmetry splitting. Unfortunately, it soon become obvious that these lines could not be fit with our earlier Hamiltonian, which could not model the rotational dependence of the torsional splitting into the asymmetric top limit. Additionally, in this much more complete data set, many of the levels are so highly mixed that their labeling becomes ambiguous, resulting in an unstable analysis. Without an analysis that provides predictions on the order of $\sim$1 MHz accuracy, we could not bootstrap the assignments very far into the asymmetric top limit due to several other unassigned rotational transitions in ν_3, ν_4, $3\nu_9$, $\nu_6 + \nu_7$, and ν_2 vibrational states, all of which have similar intensities to the transitions we were interested in. Consequently, we needed to adopt a Hamiltonian that could model the rotational dependence of the torsional splitting.

The new internal axis system (IAS) Hamiltonian includes a Fourier expansion of spectroscopic parameters in terms of $\cos(\pi\rho K)$ (*14*). To initially generate the IAS Hamiltonian, we used the experimentally determined equilibrium structure from Cox *et al*. (*15*) and the potential barrier to internal rotation from Perrin *et al*. (16) as inputs for a series of programs written by Pickett (*14*), MOIAM and IAMCALC. As part of the output, these programs determined the first order parameters for the IAS Hamiltonian and generated the constants ρ, E_ρ, A, B, C, and D_{ab} for the $2\nu_9$ vibrational state. With NO_2 being considered the top and OH the frame, symmetry considerations allowed both even and odd K_a to be conveniently labeled as belonging to the same vibrational state. The initial values for the centrifugal distortion and vibrational resonance terms were used from our previous work (*9*). However, it should be pointed out that a direct comparison of the fitted parameters between our early work and this work should not be made since this work does not use a principal axis system Hamiltonian. With the initial set of rotational and torsional parameters, it was straightforward to get the previously measured transitions in the symmetric top limit and initial assignments of transitions with asymmetry splitting fitted to their experimental uncertainties.

With the IAS Hamiltonian, the assignment and analysis of the spectrum continued with the program SPFIT (*13*) and the effective vibration–rotation–torsion Hamiltonian had the form of a 2×2 block matrix. The diagonal operators consisted of a Watson-type Hamiltonian in the A-reduction and I^r representation (*17*), rotated to an internal axis system, along with a Fourier series expansion of individual elements of the Hamiltonian. The

Hamiltonian can be expressed as

$$H_{vv} = H^R_{vv} + H^\tau_{vv} \quad [1]$$

$$H^R_{vv} = E^v + A^v J_a^2 + B^v J_b^2 + C^v J_c^2 + D^v_{ab}[J_a, J_b]_+ - \Delta^v_J J^4 - \Delta^v_{JK} J^2 J_a^2 - \Delta^v_K J_a^4 - \delta^v_k\left[J_a^2, J_{bc}^2\right]_+ - \delta^v_J\left[J^2, J_{bc}^2\right]_+ + D^v_{abJ} J^2[J_a, J_b]_+ + D^v_{abK}\left[J_a^2, [J_a, J_b]_+\right]_+ + \cdots \quad [2]$$

$$\left\langle K, v\middle|H^\tau_{vv}\middle|K', v\right\rangle = \left\langle K, v\middle|E^v_\rho + E_{\rho J} J^2 + E_{\rho K} J_a^2 + 2E_{\rho\pm} J_{bc}^2 + E_{\rho Dab}[J_a, J_b]_+ + E_{\rho JJ} J^4 + 2E_{\rho\pm J} \times \left[J^2, J_{bc}^2\right]_+\middle|K', v\right\rangle \cdot \cos\left(\pi\rho\frac{K+K'}{2}\right). \quad [3]$$

Off-diagonal $H_{vv'}$ operators included both Fermi- and Coriolis-type terms with a corresponding Fourier series expansion terms and can be expressed as

$$H_{vv'} = H^F_{vv'} + H^{F\tau}_{vv'} + H^C_{vv'} \quad [4]$$

$$H^F_{vv'} = F_0 + F_J J^2 + F_K J_a^2 + 2F_\pm J_{bc}^2 + F_{JJ} J^4 + F_{JK} J^2 J_a^2 + 2\left[F_{\pm J} J^2 + F_{\pm K} J_a^2 + F_{\pm JK} J^2 J_a^2 + F_{\pm JKK} J^2 J_a^4, J_{bc}^2\right]_+ \quad [5]$$

$$\langle K, v|H^{F\tau}|K', v'\rangle = \left\langle K, v\middle|F_{\rho 0} + 2F_{\rho\pm} J_{bc}^2\middle|K', v'\right\rangle \cdot \cos\left(\pi\rho\frac{K+K'}{2}\right) \quad [6]$$

$$H^C_{vv'} = (C_{ab} + C_{abJ} J^2)[J_a, J_b]_+, \quad [7]$$

where

$$J_{bc}^2 = J_b^2 - J_c^2 \quad [8]$$

$$[A, B]_+ = AB + BA. \quad [9]$$

A difficulty in the analysis occurs when the torsional and asymmetry splittings are similar ($\sim$50 MHz) and is related to the rotational energy level labeling and the strong Fermi resonance. When the Hamiltonian was diagonalized, vibrational assignments of the energy levels were made using the projection of the eigenvectors onto the vibrational states. Once all of the vibrational assignments were made, the energy levels were then sorted in ascending order and the normal asymmetric rotor labeling was assigned (*13*). The large Fermi resonance term, F_0, which was the focus of interest in our early work (*7*), leads to a fundamental 59/41 percent mixing of the vibrational wave functions. When the asymmetric and torsional splittings are similar, the percent mixing between the two vibrational states is near 50/50 and the vibrational assignments (and therefore the rotational assignments) are very sensitive to slight adjustments of spectroscopic parameters. This caused the assignments of certain transitions with $J \geq 28$ to become ambiguous and unstable and the assigned rotational label needed to be changed from one iteration of the fit to the next. While this problem did not degrade the quality of the fit, it did become inconvenient. This problem was avoided by removing the fundamental Fermi interaction term, F_0, and using a set of torsional parameters for the ν_5 vibrational state. This model is referred to as the artificial spitting analysis and resulted in stable and more conventional assignments of the transitions. Periodically, the induced splitting analysis, which included F_0 but no torsional parameters for ν_5, was updated with newly fitted transitions from the artificial splitting analysis. Both models fit the observed mm/submm-wave transitions to the experimental accuracy with the same number of parameters.

As pointed out in the previous paragraph, the rotational energy levels follow the normal asymmetric rotor labeling scheme. This differs from our early work (*9*), as well as that of Coudert and Perrin (*8*), where the lower energy level in the symmetric top limit would be assigned to the even K_a rotational level due to the torsional splitting. The transitions from our early paper have been relabeled for this paper.

IV. RESULTS AND DISCUSSION

Tables 1 through 3 show the transitions measured in this work and their residuals in the artificial splitting analysis. The overall rms deviation of the fit to these data and the data from our earlier work (*9*) is 0.097 MHz in the artificial splitting analysis and 0.098 MHz in the induced splitting analysis. Each analysis has 56 adjustable spectroscopic parameters and contains the same 2317 mm/submm-wave transitions, all weighted equally with a 100 kHz experimental uncertainty. Table 4 shows the spectral parameters derived from artificial splitting and the induced splitting analyses. In each analysis, the band center for ν_5 was fixed at the value determined by Ref. (*8*). The initial value for the internal axis system parameter ρ was based on the structure of the molecule, as discussed previously, and then determined empirically by adjusting this parameter until the rms deviation of the analysis was minimized. The results of the artificial splitting analysis, including all measured transitions and rotational assignments, are available as supplementary data at the journal's home page.

Table 4 shows the first order spectroscopic parameters, E_ρ, A, B, C, and D_{ab}, to be significantly different between the two analyses. This difference is due to large correlation coefficients between the parameters in the induced spitting analysis that is caused by the F_0 Fermi term. A better comparison of the constants can be made by noting the agreement between the average values of the rotational constants for each analysis, as shown in Table 5. Additionally, there is agreement in the

TABLE 1

Newly Observed Millimeter-/Submillimeter-Wave Transitions in the $\nu_5 = 1$ Vibrational State

J'	K'_a	K'_c	J''	K''_a	K''_c	ν(MHz)	$o-c$[a]	J'	K'_a	K'_c	J''	K''_a	K''_c	ν(MHz)	$o-c$[a]	J'	K'_a	K'_c	J''	K''_a	K''_c	ν(MHz)	$o-c$[a]
25	19	7	25	17	8	89656.661	-65	28	18	10	28	18	11	125150.566	11	10	0	10	9	1	9	131063.572	-16
28	22	7	28	21	8	89683.673	-38	28	18	10	28	17	11	125182.833	-4	15	6	10	15	4	11	131084.211	-76
20	14	7	20	12	8	89895.597	-19	28	19	10	28	18	11	125292.205	-14	9	1	8	8	2	7	131107.922	-21
19	12	7	19	12	8	90004.598	-2	5	5	1	4	4	0	125295.128	-1	7	4	4	6	4	3	131110.295	0
27	19	8	27	19	9	91103.308	0	28	19	10	28	17	11	125324.453	-49	9	2	8	8	1	7	131177.225	-3
17	10	7	17	10	8	91579.160	2	27	17	10	27	17	11	126064.280	-26	8	2	6	7	2	5	131197.458	-33
29	23	7	29	22	8	91629.156	-59	27	17	10	27	16	11	126081.462	6	8	3	6	7	3	5	131198.050	12
15	9	7	15	8	8	92557.236	45	27	18	10	27	17	11	126165.435	-25	35	24	11	35	23	12	131214.274	0
15	8	7	15	7	8	92574.368	23	27	18	10	27	16	11	126182.619	9	8	3	6	7	2	5	131231.692	-3
14	7	7	14	6	8	92903.832	-21	33	29	4	33	28	5	126834.385	-55	30	28	2	30	27	3	131248.676	-113
14	8	7	14	7	8	92910.010	-1	26	16	10	26	16	11	126880.496	-19	29	19	11	29	18	12	138575.533	48
5	3	3	4	3	2	93171.515	70	26	17	10	26	16	11	126898.144	34	29	18	11	29	17	12	138588.239	-75
13	7	7	13	6	8	93181.515	-16	26	16	10	26	15	11	126903.873	-40	6	5	2	5	4	1	138596.656	73
13	6	7	13	5	8	93184.345	-27	26	17	10	26	15	11	126921.514	6	29	19	11	29	17	12	138597.778	44
12	5	7	12	4	8	93403.980	70 *d*	25	15	10	25	15	11	127553.646	2	28	17	11	28	17	12	139279.528	-9
5	2	3	4	2	2	94524.832	-8	25	15	10	25	14	11	127575.228	9	46	33	13	46	33	14	139288.107	217
25	17	8	25	17	9	97172.890	-50	25	16	10	25	15	11	127592.121	-49	28	17	11	28	16	12	139300.364	5
28	21	8	28	20	9	97199.263	-88	25	16	10	25	14	11	127613.716	-30	28	18	11	28	17	12	139311.797	-23
32	23	9	32	23	10	98118.627	137	39	30	9	39	28	12	127666.807	22	28	18	11	28	16	12	139332.632	-9
32	25	8	32	24	9	98121.976	-72	43	33	11	43	32	12	127676.069	145	5	5	0	4	3	1	139421.141	154
26	19	8	26	18	9	98605.873	-89	36	28	9	36	26	10	127684.508	-77	42	31	12	42	29	13	139685.219	82
28	21	8	28	19	9	98840.641	-82	25	21	5	25	19	6	127686.877	-78	27	16	11	27	16	12	139930.497	-21
19	12	8	19	11	9	104029.198	-20	26	26	0	26	25	1	127915.580	174	27	17	11	27	16	12	139947.678	10
18	11	8	18	10	9	104492.960	-16	26	26	1	26	25	2	127938.546	114	27	16	11	27	15	12	139952.110	-29
18	10	8	18	9	9	104508.455	-2	24	14	10	24	14	11	128163.170	-4	27	17	11	27	15	12	139969.296	7
17	9	8	17	8	9	104908.921	-9	24	15	10	24	14	11	128179.191	46	44	33	12	44	31	13	140100.576	158
17	10	8	17	9	9	104913.980	-14	24	14	10	24	13	11	128186.291	-48	41	30	12	41	28	13	140448.293	29
16	9	8	16	8	9	105253.485	-20	23	13	10	23	13	11	128682.848	-18	26	15	11	26	15	12	140499.268	-11
16	8	8	16	7	9	105256.228	-19	28	23	6	28	21	7	128696.419	-26	26	15	11	26	14	12	140521.218	-19
15	7	8	15	6	9	105540.238	-37 *d*	23	13	10	23	12	11	128706.591	-11	26	16	11	26	15	12	140522.658	-19
13	6	8	13	5	9	105967.850	-53	23	14	10	23	13	11	128708.831	-23	26	16	11	26	14	12	140544.578	-57
13	5	8	13	4	9	105968.396	-11	36	25	11	36	25	12	128726.095	-28	19	17	2	19	15	5	140651.111	54
6	3	4	5	3	3	106178.142	-12	38	28	11	38	27	12	128730.684	27	39	27	12	39	28	11	140871.137	-43
6	2	4	5	2	3	106368.919	-10	23	14	10	23	12	11	128732.558	-31	25	14	11	25	14	12	141007.558	-14
14	5	9	14	5	10	118484.238	-14	39	30	10	39	29	11	128905.243	17	25	15	11	25	14	12	141029.138	-9
14	6	9	14	5	10	118515.732	-21	36	25	11	36	24	12	128982.803	-90	25	14	11	25	13	12	141030.248	-17
14	5	9	14	4	10	118516.330	-15	22	13	10	22	12	11	129166.055	-10	39	27	12	39	27	13	141034.452	-22
14	6	9	14	4	10	118547.824	-23	22	12	10	22	11	11	129167.713	-27	25	15	11	25	13	12	141051.808	-32
9	0	9	8	1	8	118581.070	-12	22	13	10	22	11	11	129190.811	-49	40	29	12	40	28	13	141141.234	-2
9	0	9	8	0	8	118616.181	2 *d*	31	25	7	31	23	8	129344.173	-6	24	13	11	24	13	12	141456.329	-12
8	1	7	7	2	6	118626.142	-12	39	30	9	39	27	12	129389.896	64	24	14	11	24	12	12	141503.019	7
13	4	9	13	4	10	118626.900	-33	48	35	13	48	34	14	129519.073	-120	40	29	12	40	27	13	141529.816	15
9	1	9	8	0	8	118651.299	22	21	11	10	21	11	11	129541.843	10	23	13	11	23	12	12	141877.228	-52
13	5	9	13	4	10	118659.248	-28	21	12	10	21	10	11	129593.057	-53	23	12	11	23	11	12	141877.980	-4
13	4	9	13	3	10	118659.845	-8	38	28	11	38	26	12	129661.950	22	45	34	12	45	32	13	141991.342	-6
8	1	7	7	1	6	118660.904	2 *d*	28	27	2	28	26	3	129858.326	-76	39	28	12	39	27	13	142757.547	24
15	14	1	15	12	4	118663.137	275	37	27	11	37	26	12	129866.294	-16	35	28	8	35	26	9	142966.514	11
7	2	5	6	3	4	118690.933	75	40	30	11	40	28	12	129872.120	62	38	26	12	38	25	13	143095.313	-30
13	5	9	13	3	10	118692.169	-27	20	10	10	20	10	11	129889.338	-12	29	24	6	29	22	7	143142.974	39
8	2	7	7	1	6	118695.671	22	41	33	9	41	32	10	129894.020	341	32	26	7	32	24	8	143174.952	22
7	3	5	6	3	4	118724.539	24	5	5	0	4	4	1	129901.385	-23	16	5	11	16	5	12	143550.049	-11
7	2	5	6	2	4	118729.448	-23	20	11	10	20	10	11	129915.350	-33	16	5	11	16	4	12	143581.660	9
39	29	11	39	27	12	118734.811	22	20	10	10	20	9	11	129916.166	-27	9	2	7	8	3	6	143639.815	-11
7	3	5	6	2	4	118763.109	-19	20	11	10	20	9	11	129942.188	-39	9	2	7	8	2	6	143673.997	-1 *d*
35	27	9	35	25	10	120225.820	94	37	27	11	37	25	12	130421.887	-15	15	4	11	15	4	12	143680.183	-19
16	14	2	16	12	5	120250.851	-52	42	30	12	42	30	13	130641.400	35	9	3	7	8	2	6	143708.179	9
6	3	3	5	3	2	120348.079	-24	16	6	10	16	6	11	130860.766	-13	8	4	5	7	4	4	143755.735	14
6	4	3	5	3	2	120968.961	34	16	7	10	16	6	11	130890.997	-50	14	3	11	14	3	12	143790.760	-25
4	4	1	3	2	2	124093.911	111	16	6	10	16	5	11	130891.676	-21	8	3	5	7	3	4	143803.359	28
38	29	10	38	27	11	124104.706	132	16	7	10	16	5	11	130921.886	-79	32	20	12	32	20	13	150265.564	-96
6	5	2	5	5	1	124370.304	-140	15	5	10	15	5	11	131021.231	-6	32	21	12	32	20	13	150276.044	39
43	31	12	43	31	13	125149.298	71	35	24	11	35	24	12	131041.220	-6	32	20	12	32	19	13	150288.232	-104

[a] Observed − calculated ($o-c$) are given in kHz. All experimental uncertainties are 100 kHz. An index *d* after the $o-c$ indicates an unresolvable symmetric top limit doublet with the $K_a + 1$ levels not listed in the table. An index # also indicated an unresolvable doublet, but in the asymmetric top limit involving levels K_c and $K_c + 1$.

TABLE 1—*Continued*

J'	K_a'	K_c'	J''	K_a''	K_c''	ν(MHz)	$o-c^a$	J'	K_a'	K_c'	J''	K_a''	K_c''	ν(MHz)	$o-c^a$	J'	K_a'	K_c'	J''	K_a''	K_c''	ν(MHz)	$o-c^a$
48	36	13	48	34	14	150479.589	-100	9	3	6	8	4	5	156192.702	-14	19	6	13	19	6	14	168446.532	-5
45	33	13	45	31	14	150569.619	110	16	4	12	16	4	13	156200.010	15	25	21	4	25	19	7	168523.132	-68
43	30	13	43	30	14	150724.525	7	9	3	6	8	3	5	156230.584	17	10	3	7	9	4	6	168659.857	-128
43	30	13	43	29	14	150996.925	26	9	4	6	8	3	5	156264.910	164	10	4	7	9	4	6	168693.604	50
31	19	12	31	19	13	151009.389	-17	15	3	12	15	3	13	156310.282	11	10	3	7	9	3	6	168694.114	-49
31	19	12	31	18	13	151030.703	10	15	4	12	15	2	13	156376.040	60	10	4	7	9	3	6	168727.729	-3
31	20	12	31	19	13	151038.383	-26	14	3	12	14	1	13	156472.580	35	9	5	5	8	5	4	168778.299	0
31	20	12	31	18	13	151059.689	-6	13	1	12	13	1	13	156486.200	-4	17	5	13	17	3	14	168779.429	-23
44	32	13	44	31	14	151281.542	56	40	28	13	40	26	14	157017.338	50	43	29	14	43	29	15	168801.111	-107
30	18	12	30	18	13	151690.364	-61	8	4	4	7	4	3	157216.400	-13	9	5	5	8	4	4	169000.431	-84
44	32	13	44	30	14	151695.462	48	5	4	2	4	2	3	157218.777	-63	6	6	0	5	4	1	169163.721	-69
30	19	12	30	18	13	151709.143	19	48	34	14	48	34	15	157382.238	204	22	4	18	22	4	19	231363.235	12
30	18	12	30	17	13	151711.723	-27	39	32	7	39	29	10	157414.827	95	22	5	18	22	4	19	231393.485	-122
30	19	12	30	17	13	151730.505	55	8	5	4	7	4	3	157438.530	-100	22	4	18	22	3	19	231394.853	55
5	5	1	4	3	2	151865.938	-85	42	33	10	42	31	11	157694.979	67	21	4	18	21	3	19	231418.487	-108
6	6	1	5	5	0	151977.708	-5	39	27	13	39	26	14	158005.690	-13	21	4	18	21	2	19	231450.777	-187
29	17	12	29	17	13	152295.944	-31	39	27	13	39	25	14	158048.235	-59	23	6	18	23	5	19	231462.267	-280
29	17	12	29	16	13	152317.183	-5	45	35	11	45	33	12	158097.621	-134	23	5	18	23	4	19	231463.950	-187
29	18	12	29	17	13	152318.203	-21	39	28	11	39	26	14	158169.164	165	20	2	18	20	2	19	231480.827	-179
29	18	12	29	16	13	152339.442	4	39	28	11	39	25	14	158211.535	-54	20	3	18	20	2	19	231513.134	-290
49	37	13	49	35	14	152710.722	-156	34	21	13	34	21	14	162821.444	-15	20	2	18	20	1	19	231514.551	178
43	31	13	43	30	14	152731.496	-21	33	20	13	33	20	14	163514.485	-11	20	3	18	20	1	19	231546.945	154
28	16	12	28	16	13	152842.095	52	33	21	13	33	20	14	163535.517	-24	12	7	6	11	6	5	231597.762	174
28	17	12	28	16	13	152862.915	52	33	20	13	33	19	14	163536.924	-38	25	8	18	25	6	19	231971.770	-145
28	16	12	28	15	13	152863.575	83	33	21	13	33	19	14	163558.020	13	26	9	18	26	7	19	232373.793	45
28	17	12	28	15	13	152884.336	23	32	19	13	32	19	14	164138.125	-21	45	27	18	45	26	19	232627.043	73
43	31	13	43	29	14	153003.901	1	32	19	13	32	18	14	164160.018	-9	45	28	18	45	26	19	232654.589	-81
42	29	13	42	29	14	153071.239	-111	32	20	13	32	19	14	164160.809	-12	11	10	2	10	10	1	232764.958	-250
42	29	13	42	28	14	153171.810	-59	32	20	13	32	18	14	164182.700	-2	27	9	18	27	9	19	232793.409	112
7	6	1	6	6	0	153176.936	-214	31	18	13	31	18	14	164704.624	-32	27	10	18	27	9	19	232820.706	311
27	15	12	27	15	13	153331.090	34	31	19	13	31	18	14	164725.960	16	27	9	18	27	8	19	232825.204	254
27	15	12	27	14	13	153352.871	68 *d*	31	18	13	31	17	14	164726.180	-33	27	10	18	27	8	19	232852.267	220
27	16	12	27	14	13	153374.592	41	31	19	13	31	17	14	164747.502	2	44	26	18	44	25	19	233297.872	285
26	14	12	26	14	13	153769.684	76	30	17	13	30	17	14	165217.505	-8	44	27	18	44	26	19	233300.011	335
26	15	12	26	14	13	153791.585	19	30	17	13	30	16	14	165238.893	-6 *d*	28	11	18	28	10	19	233339.379	247
26	14	12	26	13	13	153792.125	27	30	18	13	30	16	14	165260.293	7	28	10	18	28	9	19	233344.330	189
26	15	12	26	13	13	153814.086	30	29	16	13	29	16	14	165682.447	-11	28	11	18	28	9	19	233371.286	237
25	13	12	25	13	13	154161.977	31	29	17	13	29	16	14	165703.631	-39	11	9	3	10	9	2	233730.248	278
25	14	12	25	13	13	154184.658	19	29	16	13	29	15	14	165704.038	19	29	11	18	29	11	19	233835.847	128
25	13	12	25	12	13	154185.258	51	29	17	13	29	15	14	165725.225	-5	29	12	18	29	11	19	233862.447	-135
42	30	13	42	29	14	154273.196	-18	28	15	13	28	15	14	166103.573	-13	43	25	18	43	25	19	233865.259	-59
42	30	13	42	28	14	154373.756	22	28	16	13	28	14	14	166146.907	-21	29	11	18	29	10	19	233867.604	-127
24	12	12	24	12	13	154512.488	67	7	6	2	6	5	1	166201.415	19	43	25	18	43	24	19	233890.788	-173
24	13	12	24	11	13	154560.070	-3	45	32	14	45	30	15	166357.277	60	43	26	18	43	25	19	233892.641	-180
23	11	12	23	11	13	154824.858	72	27	14	13	27	14	14	166484.800	-22	29	12	18	29	10	19	233894.498	-97
23	12	12	23	10	13	154874.340	-3	27	15	13	27	14	14	166506.740	43	43	26	18	43	24	19	233918.314	-150
6	6	0	5	5	1	154937.623	-29	27	14	13	27	13	14	166507.151	-87	30	13	18	30	12	19	234359.773	325
41	28	13	41	28	14	155000.720	-8	27	15	13	27	13	14	166529.087	-26	42	24	18	42	24	19	234382.300	331
41	28	13	41	27	14	155095.162	-68	26	13	13	26	13	14	166829.582	8	30	13	18	30	11	19	234391.659	289
22	10	12	22	10	13	155102.539	45	26	14	13	26	12	14	166875.144	-27	42	24	18	42	23	19	234407.798	-43
22	11	12	22	9	13	155154.060	-17	25	12	13	25	12	14	167140.911	-3	42	25	18	42	24	19	234409.495	60
21	9	12	21	9	13	155348.720	39	25	13	13	25	11	14	167188.078	-27	31	13	18	31	13	19	234778.607	147
21	10	12	21	8	13	155402.359	-1	44	30	14	44	29	15	167346.445	-24	27	8	19	27	7	20	234799.308	140
20	8	12	20	8	13	155566.269	44	24	11	13	24	11	14	167421.632	18	31	14	18	31	13	19	234805.714	190
20	9	12	20	7	13	155622.024	0	24	12	13	24	10	14	167470.607	-9	31	13	18	31	12	19	234810.191	76
41	29	13	41	28	14	155626.405	-30	23	10	13	23	10	14	167674.191	6	41	23	18	41	23	19	234822.578	376
41	29	13	41	27	14	155720.883	-54	44	31	14	44	30	15	167688.648	-14	27	9	19	27	7	20	234831.064	244
19	7	12	19	7	13	155757.780	7	23	11	13	23	9	14	167725.126	-28	31	14	18	31	12	19	234837.532	353
8	5	4	7	5	3	155914.620	-36	44	31	14	44	29	15	167760.357	-39	41	24	18	41	22	19	234876.006	152
18	6	12	18	6	13	155925.780	10	22	10	13	22	9	14	167927.050	-20	32	14	18	32	14	19	235156.536	-113
17	5	12	17	5	13	156072.501	24	21	8	13	21	8	14	168103.958	6	32	15	18	32	14	19	235183.708	-165
7	5	2	6	5	1	156089.605	-6	21	9	13	21	7	14	168159.074	-27	40	22	18	40	22	19	235185.472	-121
54	39	15	54	39	16	156116.074	-73	22	20	2	22	18	5	168264.235	-156	32	14	18	32	13	19	235187.926	31
17	6	12	17	4	13	156134.480	34	20	7	13	20	7	14	168285.193	-23	33	15	18	33	15	19	235456.501	21

TABLE 1—*Continued*

J'	K_a'	K_c'	J''	K_a''	K_c''	ν(MHz)	$o-c^a$		J'	K_a'	K_c'	J''	K_a''	K_c''	ν(MHz)	$o-c^a$		J'	K_a'	K_c'	J''	K_a''	K_c''	ν(MHz)	$o-c^a$	
39	21	18	39	21	19	235471.157	-12		20	1	19	19	2	18	268386.184	127		21	4	18	20	3	17	305896.677	36	
33	16	18	33	15	19	235483.672	-183		21	1	21	20	0	20	268409.750	9		20	4	16	19	5	15	305899.140	43	
33	15	18	33	14	19	235487.130	-74		18	3	15	17	4	14	268457.762	-56		19	5	14	18	6	13	305951.047	-54	
39	21	18	39	20	19	235498.365	-104	*d*	19	3	17	18	2	16	268484.567	265		20	5	16	19	4	15	305960.543	-43	
33	16	18	33	14	19	235514.417	-163		18	4	15	17	3	14	268521.952	161		18	6	12	17	7	11	306016.783	15	
39	22	18	39	20	19	235525.511	-256		16	5	11	15	6	10	268559.426	53		18	7	12	17	6	11	306076.322	-18	
34	16	18	34	16	19	235672.115	-106		17	5	13	16	4	12	268564.164	46		17	7	10	16	8	9	306129.205	-5	
38	20	18	38	20	19	235677.358	-107		16	5	11	15	5	10	268590.379	-57	*d*	17	7	10	16	7	9	306158.721	27	*d*
34	17	18	34	16	19	235699.451	-264		16	6	11	15	5	10	268621.576	77		17	8	10	16	7	9	306188.207	28	
34	16	18	34	15	19	235702.037	-316		15	6	9	14	7	8	268663.476	78		22	2	20	21	2	19	306319.189	-1	*d*
38	20	18	38	19	19	235704.741	-318	*d*	15	7	9	14	6	8	268724.888	218		11	10	1	10	8	2	307117.887	-96	
34	17	18	34	15	19	235729.795	-53		42	21	21	42	21	22	268967.526	183		15	9	6	14	9	5	308171.226	176	
38	21	18	38	19	19	235732.725	71		14	7	7	13	7	6	268989.031	222		15	10	6	14	9	5	308523.108	231	
35	17	18	35	17	19	235801.659	44		41	20	21	41	19	22	269089.452	177	*d*	12	10	2	11	9	3	308902.458	209	
37	19	18	37	19	19	235802.677	40		24	3	21	24	3	22	269131.209	19		39	15	25	39	13	26	317386.966	-95	
35	18	18	35	17	19	235829.025	-160		27	7	21	27	5	22	269228.579	42		38	14	25	38	13	26	317563.999	32	
36	18	18	36	18	19	235844.543	-110		39	18	21	39	17	22	269253.279	4	*d*	38	13	25	38	12	26	317565.364	27	
11	7	4	10	7	3	235849.767	-243		28	8	21	28	6	22	269257.878	-10		37	12	25	37	12	26	317730.772	-20	
36	19	18	36	18	19	235872.255	-1		39	19	21	39	17	22	269260.731	-7		37	13	25	37	11	26	317758.310	-53	
36	18	18	36	17	19	235873.395	-112		30	9	21	30	9	22	269282.950	-45		10	5	5	9	3	6	317855.343	22	
36	19	18	36	17	19	235901.201	91		29	9	21	29	7	22	269290.211	-20		10	6	5	9	4	6	317913.375	251	
11	9	2	10	9	1	242592.875	38		30	10	21	30	8	22	269322.529	1		36	12	25	36	10	26	317932.060	-81	
9	8	1	8	6	2	245935.810	39		31	11	21	31	10	22	269333.195	109		13	11	3	12	10	2	317957.051	-72	
9	7	2	8	5	3	246053.985	19		31	10	21	31	9	22	269335.809	17		23	2	21	22	3	20	318082.445	0	
12	9	4	11	9	3	252770.938	167		37	16	21	37	16	22	269343.999	-107		23	2	21	22	2	20	318114.179	-63	*d*
12	11	2	11	11	1	253796.028	24		32	11	21	32	11	22	269345.725	184		23	3	21	22	2	20	318145.957	-83	
12	11	1	11	11	0	254613.031	-43		37	17	21	37	16	22	269349.802	114		22	3	19	21	3	18	318171.269	-57	*d*
17	3	14	16	4	13	255984.452	-207		36	15	21	36	15	22	269369.482	49		22	4	19	21	3	18	318202.625	-176	
18	3	16	17	2	15	256010.976	-176		35	14	21	35	14	22	269380.704	74		25	1	25	24	0	24	318308.750	-76	
14	6	8	13	6	7	256259.691	-76		33	12	21	33	11	22	269381.832	40		21	4	17	20	5	16	318346.422	-3	
14	7	8	13	7	7	256261.465	-1		36	16	21	36	14	22	269384.745	64		21	5	17	20	4	16	318407.402	-109	
13	7	6	12	7	5	256882.473	-42		33	13	21	33	11	22	269393.731	172		20	6	15	19	5	14	318469.017	-178	
28	8	20	28	8	21	258519.758	-45		35	15	21	35	13	22	269399.172	92		19	6	13	18	7	12	318472.231	-78	
28	9	20	28	8	21	258539.130	-81		34	14	21	34	12	22	269401.708	88		19	6	13	18	6	12	318501.616	-163	*d*
28	8	20	28	7	21	258542.594	-22		12	9	3	11	9	2	269574.854	-10		19	7	13	18	6	12	318531.113	-136	
28	9	20	28	7	21	258562.005	-19		10	8	2	9	6	3	270311.222	-97		18	7	11	17	8	10	318566.665	-101	
29	9	20	29	9	21	258707.812	108		13	10	4	12	10	3	276070.844	-105		18	8	11	17	7	10	318624.912	-75	
29	10	20	29	9	21	258724.767	48		21	1	20	20	2	19	280862.281	-234		17	8	9	16	8	8	318788.647	-125	
29	9	20	29	8	21	258728.545	143		20	3	18	19	2	17	280950.321	-339		17	9	9	16	9	8	318790.300	27	
29	10	20	29	8	21	258745.387	-29		18	4	14	17	5	13	280970.756	-130		16	10	7	15	10	6	319209.651	69	
30	10	20	30	10	21	258866.850	32		19	4	16	18	3	15	280991.535	-51		15	10	5	14	10	4	325518.101	3	
30	11	20	30	9	21	258899.690	-235		17	5	12	16	6	11	281024.028	2		43	17	26	43	17	27	329016.352	-87	
31	11	20	31	11	21	258997.876	-161		16	6	10	15	6	9	281139.341	-162	*d*	43	17	26	43	16	27	329026.263	-153	*d*
31	12	20	31	11	21	259010.145	-75		16	7	10	15	6	9	281169.891	-34		43	18	26	43	16	27	329036.365	-25	
31	11	20	31	10	21	259014.059	-248		15	8	8	14	8	7	281324.255	-17		15	11	5	14	10	4	329051.116	-153	
32	12	20	32	12	21	259102.157	-165		15	7	8	14	7	7	281330.629	149		42	16	26	42	16	27	329253.689	47	
32	13	20	32	12	21	259112.284	160		15	8	8	14	7	7	281361.047	-81		42	16	26	42	15	27	329263.297	53	*d*
32	13	20	32	11	21	259125.977	-154		21	2	19	20	3	18	293312.206	-227		42	17	26	42	15	27	329272.919	72	
33	14	20	33	13	21	259187.912	-169		22	1	21	21	2	20	293338.237	-8		11	11	1	10	9	2	329411.928	194	
33	13	20	33	12	21	259192.246	-89		21	3	19	20	2	18	293377.020	-201		41	15	26	41	15	27	329479.893	119	
34	15	20	34	14	21	259239.175	204		20	3	17	19	4	16	293391.462	-39		41	15	26	41	14	27	329489.765	132	*d*
34	14	20	34	13	21	259243.066	-64		22	2	21	21	1	20	293404.663	52		41	16	26	41	14	27	329499.358	-135	
52	31	21	52	30	22	266682.035	111	*d*	19	4	15	18	5	14	293437.672	-175		13	12	2	12	11	1	329521.287	97	
12	9	4	11	8	3	266852.705	-51		20	4	17	19	3	16	293454.664	-29		12	9	3	11	7	4	329606.958	10	
51	30	21	51	29	22	267025.123	64	*d*	18	5	13	17	6	12	293488.448	-37		39	13	26	39	13	27	329900.994	-137	
50	30	21	50	28	22	267367.349	3		19	5	15	18	4	14	293499.774	-23		39	14	26	39	13	27	329912.405	-75	
49	28	21	49	27	22	267627.917	-238	*d*	17	6	11	16	7	10	293561.539	48		39	13	26	39	12	27	329913.683	-25	
48	27	21	48	27	22	267866.171	-4		17	6	11	16	6	10	293591.811	213	*d*	39	14	26	39	12	27	329924.960	-97	
47	26	21	47	25	22	268127.460	-278		21	3	18	20	4	17	305833.737	-20		37	11	26	37	11	27	330285.182	-156	
47	27	21	47	26	22	268128.574	-141		24	1	24	23	0	23	305835.362	90		37	12	26	37	11	27	330299.737	-137	
47	27	21	47	25	22	268150.584	-288		23	2	22	22	1	21	305879.345	16		37	11	26	37	10	27	330301.371	8	
37	12	26	37	10	27	330315.922	23		25	1	24	24	2	23	330760.826	113		22	5	18	21	4	17	330808.351	-24	
36	11	26	36	9	27	330499.153	9		24	2	22	23	3	21	330772.303	19		16	10	6	15	11	5	330824.592	-5	
26	0	26	25	1	25	330713.588	132		26	1	26	25	0	25	330781.568	55		25	2	24	24	1	23	330826.277	-46	

TABLE 1—*Continued*

J'	K_a'	K_c'	J''	K_a''	K_c''	ν(MHz)	$o-c^a$	J'	K_a'	K_c'	J''	K_a''	K_c''	ν(MHz)	$o-c^a$	J'	K_a'	K_c'	J''	K_a''	K_c''	ν(MHz)	$o-c^a$	
24	3	22	23	2	21	330835.520	-93	24	4	21	23	3	20	342791.542	153	38	11	28	38	9	29	355333.379	17	
21	5	16	20	6	15	330857.736	-44	23	4	19	22	5	18	342842.217	7	37	10	28	37	8	29	355535.010	120	
13	12	1	12	11	2	330895.727	67	23	4	19	22	4	18	342872.900	-31	*d*	28	0	28	27	1	27	355656.283	-118
21	6	16	20	5	15	330917.116	-44	23	5	19	22	4	18	342903.646	-7	36	8	28	36	8	29	355687.623	-216	
20	6	14	19	7	13	330925.308	-88	36	9	27	36	9	28	343064.766	-36	25	3	22	24	4	21	355696.418	37	
20	7	14	19	6	13	330983.644	-80	27	0	27	26	1	26	343185.462	65	27	1	26	26	2	25	355704.757	17	
19	7	12	18	8	11	331009.408	-67	26	1	25	25	2	24	343233.219	41	28	1	28	27	0	27	355724.139	-2	
19	7	12	18	7	11	331038.157	-82	*d*	27	1	27	26	0	26	343253.283	-12	26	2	24	25	3	23	355740.743	37
19	8	12	18	7	11	331066.856	-146	25	2	23	24	3	22	343263.491	60	25	4	22	24	3	21	355756.693	21	
18	8	10	17	8	9	331187.779	-97	*d*	22	5	17	21	6	16	343281.505	-11	27	2	26	26	1	25	355769.790	-42
18	9	10	17	8	9	331216.215	-4	25	3	23	24	2	22	343326.458	8	22	7	16	21	6	15	355860.285	0	
19	13	6	18	15	3	331489.020	94	21	6	15	20	7	14	343371.911	29	21	7	14	20	8	13	355893.997	64	
17	9	8	16	10	7	331499.850	-74	21	7	15	20	6	14	343429.709	71	20	9	12	19	8	11	356058.827	-17	
16	11	6	15	11	5	331507.473	-166	20	7	13	19	8	12	343453.283	20	19	9	10	18	10	9	356202.813	121	
17	10	8	16	10	7	331533.339	-89	19	9	11	18	8	10	343633.370	77	17	12	6	16	12	5	356254.171	-45	
17	9	8	16	9	7	331573.137	-88	28	2	27	28	1	28	344327.067	2	19	10	10	18	9	9	356258.228	163	
17	10	8	16	9	7	331606.660	-70	28	1	27	28	0	28	344328.445	-100	14	13	1	13	12	2	356626.084	58	
23	3	20	22	4	19	332017.033	48	17	10	7	16	10	6	344955.964	248	18	10	8	17	11	7	356682.395	70	
23	4	20	22	3	19	332078.700	-48	17	11	7	16	10	6	345040.663	18	24	4	20	23	5	19	358025.494	199	
15	12	3	14	12	2	332392.629	112	12	10	3	11	8	4	346911.741	122	24	5	20	23	4	19	358084.830	183	
16	10	6	15	10	5	334357.670	-100	12	11	2	11	9	3	349477.804	36	17	16	2	16	16	1	358114.589	268	
16	11	6	15	10	5	335040.900	87	12	8	4	11	6	5	349939.498	-198	17	16	1	16	16	0	358157.141	126	
13	13	1	12	12	0	335434.640	-152	53	25	28	53	25	29	351047.541	25	16	12	5	15	11	4	358365.143	-132	
13	13	0	12	12	1	335478.935	-148	53	25	28	53	24	29	351071.445	165	12	12	1	11	10	2	360187.067	-7	
15	11	4	14	11	3	337296.758	-202	53	26	28	53	25	29	351072.924	111	16	12	4	15	12	3	360254.289	-56	
16	15	2	15	15	1	337301.877	-206	13	11	2	12	9	3	351726.720	-206	17	11	6	16	11	5	360970.381	224	
16	15	1	15	15	0	337381.894	-176	51	23	28	51	22	29	351800.183	-47	14	14	1	13	13	0	361388.969	178	
12	11	1	11	9	2	339080.229	53	51	24	28	51	23	29	351801.947	125	14	14	0	13	13	1	361411.626	277	
50	23	27	50	23	28	339540.824	-161	16	13	3	15	13	2	351902.569	-124	17	15	3	16	15	2	361798.334	44	
50	23	27	50	22	28	339560.336	-86	50	22	28	50	21	29	352142.750	-181	17	12	6	16	11	5	362373.299	-259	
50	24	27	50	23	28	339561.974	-20	50	23	28	50	22	29	352144.386	-126	17	13	5	16	13	4	363930.177	322	
49	22	27	49	22	28	339870.970	-97	16	11	5	15	11	4	352245.795	-138	17	14	4	16	14	3	364979.345	61	
49	22	27	49	21	28	339888.402	-119	49	21	28	49	20	29	352472.044	217	40	12	29	40	11	30	367520.547	28	
49	23	27	49	22	28	339889.956	-120	49	22	28	49	21	29	352473.453	89	40	11	29	40	10	30	367521.883	3	
49	23	27	49	21	28	339907.353	-177	48	20	28	48	20	29	352773.351	-11	21	9	13	20	8	12	368486.713	-96	
47	20	27	47	20	28	340490.316	165	48	20	28	48	19	29	352787.478	39	35	7	29	35	6	30	368535.014	-242	
47	20	27	47	19	28	340503.965	109	48	21	28	48	20	29	352788.984	97	19	10	9	18	11	8	368958.458	0	
47	21	27	47	20	28	340505.387	136	48	21	28	48	19	29	352803.187	225	19	10	9	18	10	8	368971.074	-25	
47	21	27	47	19	28	340519.087	130	39	11	28	39	11	29	355094.200	-28	19	11	9	18	11	8	368983.411	-35	
38	11	27	38	11	28	342685.649	44	39	12	28	39	11	29	355107.994	-123	19	11	9	18	10	8	368996.026	-62	
38	12	27	38	10	28	342715.580	87	39	11	28	39	10	29	355109.715	204	25	8	17	24	8	16	417970.390	104	*d*
24	3	21	23	4	20	342731.058	69	39	12	28	39	10	29	355123.515	115	29	12	17	28	12	16	517106.514	-133	
24	3	21	23	3	20	342761.239	50	*d*	38	10	28	38	10	29	355300.602	44	20	20	1	19	19	0	517200.500	137 #

determination of the difference between the perturbed band centers, ΔE. The interstate transitions between ν_5 and $2\nu_9$ listed in Table 3, other transitions involving levels with significant mixing, and the measurement of the torsional splitting in each state allow an accurate determination of ΔE in each analysis. However, if the ν_5 band center in the induced analysis is allowed to vary by including infrared energy levels, the uncertainties in the unperturbed band centers, ΔE_0, and the Fermi constant become quite large and have values of ~48 MHz and ~9 MHz, respectively. This again is due to the large correlation (~ -0.999) between these parameters. However, even with this correlation, the determination of ΔE is not affected.

The microwave transitions for the ν_5 vibrational state include rotational quantum numbers up to $J_{max} \leq 54$ and $K_{a\,max} \leq 39$, while those for the $2\nu_9$ vibrational state include $J_{max} \leq 51$ and $K_{a\,max} \leq 37$. Figure 1 shows the locations ($J, \tau = K_a - K_c$) of the ν_5 energy levels connected by transitions in the microwave fit. This figure includes a contour map of the mixing coefficients for the ν_5 energy levels in terms of the $2\nu_9$ vibrational state wave function contributions in the artificial splitting analysis. A large region of significant mixing, where the percentage reaches 50%, is due to the $\Delta K_a = \pm 2$ Fermi interaction. A figure for $2\nu_9$ energy levels exhibits similar characteristics.

Rotational dependence of the torsional splitting is shown in Fig. 2 for $J = 45$ in the ν_5 vibrational state and was calculated from the artificial splitting analysis. The figure shows a plot of the differences between the (K_a, K_c) and $(K_a + 1, K_c)$ energy levels on two different scales; the left axis shows the torsional contribution and the right axis shows the asymmetric splitting contribution. The torsional dependence is easily recognized in the symmetric top limit. As the asymmetric splitting becomes comparable to the torsional splitting, mixing significantly effects the rotational energy level labeling and no systematic pattern is discernable. Far into the asymmetric limit, a pattern reemerges when the energy levels with (K_a, K_c) and $(K_a, K_c + 1)$ become clustered (*8*).

TABLE 2

Newly Observed Millimeter-/Submillimeter-Wave Transitions in the $\nu_9 = 2$ Vibrational State

J'	K_a'	K_c'	J''	K_a''	K_c''	ν(MHz)	$o-c$[a]	J'	K_a'	K_c'	J''	K_a''	K_c''	ν(MHz)	$o-c$[a]	J'	K_a'	K_c'	J''	K_a''	K_c''	ν(MHz)	$o-c$[a]
19	13	7	19	11	8	89928.171	23	23	13	10	23	13	11	127994.659	24	22	19	4	22	17	5	131608.324	87
25	19	7	25	17	8	90131.858	-48	41	29	12	41	29	13	128013.853	36	6	4	2	5	4	1	131845.545	28
18	11	7	18	11	8	90194.652	18	23	13	10	23	12	11	128018.211	-5	34	24	11	34	23	12	132222.709	-131
28	22	7	28	21	8	90206.380	-23	23	14	10	23	13	11	128021.462	31	27	16	11	27	16	12	139025.602	-4
18	11	7	18	10	8	90210.130	13	17	15	2	17	13	5	128050.506	29	27	16	11	27	15	12	139071.483	-23
27	19	8	27	18	9	90242.590	2	29	27	2	29	26	3	128070.441	98	27	17	11	27	16	12	139090.777	20
24	21	4	24	20	5	91447.699	-2	29	27	3	29	26	4	128079.175	56	27	17	11	27	15	12	139136.642	-14
16	9	7	16	9	8	91518.670	25	37	31	7	37	30	8	128096.204	116	7	4	3	6	5	2	139400.554	-33
16	9	7	16	8	8	91554.241	-12	37	27	11	37	26	12	128140.092	22	44	31	13	44	31	14	139427.695	30
16	10	7	16	9	8	91615.321	12	35	30	5	35	29	6	128176.487	-41	39	27	12	39	26	13	139437.758	3
16	10	7	16	8	8	91650.923	6	22	12	10	22	12	11	128467.627	-1	5	5	0	4	3	1	139608.900	204
5	3	3	4	3	2	92962.772	16	22	13	10	22	12	11	128497.220	-3	26	15	11	26	15	12	139669.073	0
6	1	5	5	1	4	93607.303	24 *d*	22	12	10	22	11	11	128498.644	-6	26	15	11	26	14	12	139678.733	-8
6	2	5	5	1	4	93657.222	39	22	13	10	22	11	11	128528.226	-18	26	16	11	26	15	12	139739.400	-7
5	2	3	4	2	2	94435.238	6	35	30	6	35	29	7	128856.035	-84	26	16	11	26	14	12	139749.058	-17
31	22	9	31	22	10	97437.702	66	31	28	3	31	27	4	128860.464	43	25	14	11	25	14	12	140246.833	40
24	16	8	24	16	9	98021.012	5	21	11	10	21	11	11	128882.785	16	25	15	11	25	13	12	140278.613	-45
24	16	8	24	15	9	98204.674	7	21	12	10	21	11	11	128912.161	-9	24	13	11	24	13	12	140717.418	9
27	20	8	27	18	9	98615.038	-21	21	11	10	21	10	11	128914.124	-4	24	13	11	24	12	12	140741.235	-18
17	9	8	17	8	9	104329.525	8	21	12	10	21	10	11	128943.498	-32	24	14	11	24	13	12	140752.936	-15
17	10	8	17	9	9	104336.505	-19	33	29	4	33	28	5	128997.128	193	24	14	11	24	12	12	140776.745	-51
16	9	8	16	8	9	104689.495	1	20	10	10	20	10	11	129237.962	11	20	18	3	20	16	4	140807.684	-37
16	8	8	16	7	9	104693.693	-5	20	11	10	20	10	11	129271.648	-51	49	35	14	49	35	15	141081.604	-132
15	7	8	15	6	9	104988.050	-6 *d*	20	10	10	20	9	11	129272.123	23	43	33	11	43	31	12	141109.034	-67
9	2	8	9	1	9	105878.135	72	20	11	10	20	9	11	129305.825	-24	23	12	11	23	12	12	141143.189	43
9	1	8	9	0	9	105879.106	21	36	26	11	36	25	12	129492.276	-121	23	13	11	23	12	12	141166.725	-2
6	3	4	5	3	3	106015.315	4	19	9	10	19	9	11	129545.119	33	23	12	11	23	11	12	141172.575	-11
6	2	4	5	2	3	106233.937	0	19	10	10	19	9	11	129579.237	-5	23	13	11	23	11	12	141196.120	-48
40	30	11	40	29	12	118494.137	64	35	24	11	35	23	12	129664.442	37	38	26	12	38	26	13	141327.146	-47
8	1	7	7	2	6	118519.608	21	37	27	11	37	25	12	129736.951	74	43	30	13	43	30	14	141388.971	-7
7	2	5	6	3	4	118522.933	-6	18	8	10	18	8	11	129805.785	9	22	11	11	22	11	12	141506.826	11
9	0	9	8	1	8	118537.474	0	18	9	10	18	7	11	129881.481	-4	22	11	11	22	10	12	141537.205	-50
8	1	7	7	1	6	118569.249	66 *d*	17	7	10	17	7	11	130027.702	15	22	12	11	22	11	12	141537.835	0
7	3	5	6	3	4	118571.308	19	17	8	10	17	6	11	130106.654	-1	22	12	11	22	10	12	141568.241	-36
7	2	5	6	2	4	118579.995	25	16	6	10	16	6	11	130213.779	-2	21	10	11	21	10	12	141824.655	16
9	0	9	8	0	8	118587.904	25 *d*	16	7	10	16	5	11	130297.073	-17	21	11	11	21	9	12	141889.097	-46
8	2	7	7	1	6	118618.829	48	15	5	10	15	5	11	130369.267	23	43	32	12	43	30	13	142027.644	162
9	1	9	8	0	8	118638.314	30	15	6	10	15	5	11	130411.948	7	20	9	11	20	9	12	142098.249	7
38	27	11	38	27	12	118669.597	70	15	5	10	15	4	11	130413.310	8	20	10	11	20	9	12	142132.397	6
6	3	3	5	3	2	120239.381	21	15	6	10	15	4	11	130456.003	4	20	9	11	20	8	12	142133.502	3
6	4	3	5	3	2	120947.843	2	14	4	10	14	4	11	130497.381	-6	44	33	12	44	31	13	142153.626	-131
6	5	2	5	5	1	123783.126	-99	14	5	10	14	4	11	130541.948	6	19	8	11	19	8	12	142333.586	8
33	26	8	33	24	9	124176.750	-276	14	4	10	14	3	11	130543.168	-14	19	9	11	19	8	12	142369.653	-40
37	26	11	37	25	12	124385.677	76	36	26	11	36	24	12	130565.899	-15	19	8	11	19	7	12	142371.050	-15
28	19	10	28	17	11	124584.536	9	14	5	10	14	3	11	130587.736	0	19	9	11	19	7	12	142407.173	-8
27	17	10	27	17	11	125246.486	26	13	3	10	13	3	11	130601.993	5	18	7	11	18	7	12	142534.489	-3
5	5	1	4	4	0	125303.041	115	13	3	10	13	2	11	130649.419	9	18	8	11	18	6	12	142612.358	-1
27	17	10	27	16	11	125311.658	48	12	2	10	12	2	11	130686.110	-39	17	6	11	17	6	12	142704.961	-19
27	18	10	27	17	11	125358.906	-31	12	3	10	12	2	11	130733.832	-1	17	7	11	17	5	12	142786.903	2
26	16	10	26	16	11	126090.287	0	11	2	10	11	1	11	130801.943	10	16	6	11	16	4	12	142934.359	13
26	17	10	26	16	11	126117.241	21	35	25	11	35	24	12	130848.428	12	37	25	12	37	25	13	142949.403	-64
26	16	10	26	15	11	126160.609	-13	11	2	10	11	0	11	130852.278	13	39	28	12	39	26	13	143409.132	-18
26	17	10	26	15	11	126187.576	22	8	2	6	7	3	5	130997.293	-28	9	2	7	8	3	6	143473.542	6
36	25	11	36	25	12	126193.534	-40	9	1	8	8	2	7	131001.729	-6	8	4	5	7	4	4	143549.046	39
25	15	10	25	14	11	126828.929	-2	10	0	10	9	1	9	131020.440	-11	8	3	5	7	3	4	143597.996	44
25	16	10	25	15	11	126866.544	12	34	23	11	34	23	12	131034.150	-48	19	17	2	19	15	5	143683.108	67
24	14	10	24	14	11	127443.620	11	8	2	6	7	2	5	131045.824	29 *d*	45	34	12	45	32	13	143703.148	-2
24	15	10	24	14	11	127464.929	4	9	1	8	8	1	7	131051.196	20 *d*	20	17	3	20	15	6	143789.395	-233
24	14	10	24	13	11	127479.132	-19	8	3	6	7	2	5	131094.296	26	36	24	12	36	23	13	150073.844	-222
24	15	10	24	13	11	127500.524	57	9	2	8	8	1	7	131100.659	41	35	32	3	35	31	4	150135.804	84
39	29	11	39	28	12	127727.163	-13	10	1	10	9	0	9	131121.241	42	35	32	4	35	31	5	150139.571	-132

[a] Observed − calculated ($o - c$) are in kHz. All experimental uncertainties are 100 kHz. An index *d* after the $o - c$ indicates an unresolvable symmetric top limit doublet with the $K_a + 1$ levels not listed in table. An index # also indicated an unresolvable doublet, but in the asymmetric top limit involving levels K_c and $K_c + 1$.

TABLE 2—*Continued*

J'	K_a'	K_c'	J''	K_a''	K_c''	ν(MHz)	$o-c$[a]	J'	K_a'	K_c'	J''	K_a''	K_c''	ν(MHz)	$o-c$[a]	J'	K_a'	K_c'	J''	K_a''	K_c''	ν(MHz)	$o-c$[a]
33	22	12	33	20	13	150266.524	74	19	8	12	19	6	13	155113.762	299	25	13	13	25	11	14	166391.168	-47
34	23	12	34	21	13	150292.446	-96	36	23	13	36	23	14	155120.694	151	24	11	13	24	11	14	166642.569	27
32	21	12	32	20	13	150467.225	19	18	6	12	18	6	13	155191.899	33	24	12	13	24	11	14	166670.334	-6
35	24	12	35	22	13	150666.834	104	18	7	12	18	5	13	155272.599	39	24	11	13	24	10	14	166671.448	-10
31	19	12	31	19	13	150684.254	25	36	23	13	36	22	14	155279.086	63	24	12	13	24	10	14	166699.197	-60
31	19	12	31	18	13	151106.338	20	36	33	3	36	32	4	155301.489	9	22	20	3	22	18	4	166785.198	-136
36	25	12	36	23	13	151147.521	-62	36	33	4	36	32	5	155303.350	-243	23	11	13	23	10	14	166937.603	16
30	18	12	30	18	13	151216.350	1	8	4	4	7	5	3	155306.384	-16	23	10	13	23	9	14	166938.894	4
31	20	12	31	18	13	151312.480	18	17	5	12	17	5	13	155324.469	11	23	11	13	23	9	14	166968.844	-27
30	19	12	30	18	13	151327.660	31	17	6	12	17	5	13	155366.093	-7	40	36	4	40	35	5	166993.368	6
30	18	12	30	17	13	151336.906	24	17	6	12	17	4	13	155409.239	8	40	36	5	40	35	6	166996.501	-2
30	19	12	30	17	13	151448.207	45	7	5	2	6	5	1	155410.040	15	46	33	14	46	31	15	167066.055	52
37	26	12	37	24	13	151567.736	40	16	4	12	16	4	13	155436.979	29	22	9	13	22	9	14	167138.719	32
40	28	13	40	27	14	151691.069	67	15	3	12	15	3	13	155531.439	7	22	10	13	22	9	14	167170.979	16
38	27	12	38	25	13	151727.446	-24	14	2	12	14	2	13	155609.940	23	22	9	13	22	8	14	167172.346	7
29	17	12	29	17	13	151750.775	10	15	4	12	15	2	13	155623.860	76	22	10	13	22	8	14	167204.574	-40
29	17	12	29	16	13	151762.982	64	39	25	15	39	25	14	155743.958	14	41	27	14	41	26	15	167215.121	53
29	18	12	29	17	13	151847.345	7	9	3	6	8	4	5	155970.445	-99	21	8	13	21	8	14	167339.574	3
29	18	12	29	16	13	151859.543	52	12	0	12	11	1	11	155985.538	17	21	9	13	21	7	14	167410.085	-19
28	16	12	28	16	13	152257.605	59	9	4	6	8	4	5	156018.628	0	20	7	13	20	7	14	167513.511	25
28	17	12	28	16	13	152285.324	93	9	3	6	8	3	5	156021.968	32	20	8	13	20	6	14	167588.525	-25
28	16	12	28	15	13	152285.684	17	9	4	6	8	3	5	156070.005	-14	19	6	13	19	6	14	167663.355	44
28	17	12	28	15	13	152313.403	52	41	29	13	41	27	14	156569.856	-193	19	7	13	19	6	14	167702.284	0
38	25	13	38	24	14	152683.126	19	5	4	2	4	2	3	156831.772	-28	19	6	13	19	5	14	167703.810	-6
27	15	12	27	15	13	152706.955	92	8	4	4	7	4	3	157064.705	31	18	5	13	18	5	14	167791.647	9
46	34	13	46	32	14	152718.633	290	22	19	3	22	17	6	157071.905	0	18	6	13	18	5	14	167832.729	0
27	15	12	27	14	13	152726.197	81	8	5	4	7	4	3	157342.604	8	18	6	13	18	4	14	167875.385	3
27	16	12	27	15	13	152752.826	63	21	17	4	21	15	7	157362.809	-69	17	5	13	17	4	14	167943.987	36
27	16	12	27	14	13	152772.060	45	40	28	13	40	26	14	157408.378	13	17	4	13	17	3	14	167945.537	7
47	35	13	47	33	14	152817.725	-211	35	22	13	35	21	14	157436.819	-46	17	5	13	17	3	14	167988.641	-17
26	14	12	26	14	13	153140.009	90	22	18	4	22	16	7	158092.238	-61	16	3	13	16	3	14	167992.969	-45
45	33	13	45	31	14	153146.776	-171	39	26	13	39	26	14	158233.234	-133	15	2	13	15	2	14	168070.186	-9
26	15	12	26	14	13	153149.659	73	20	16	4	20	14	7	158463.295	44	16	4	13	16	2	14	168084.766	10
26	14	12	26	13	13	153164.149	61	38	26	13	38	25	14	159085.896	-4	15	3	13	15	1	14	168165.655	20
26	15	12	26	13	13	153173.803	47	31	18	13	31	18	14	162796.944	3	14	2	13	14	1	14	168182.854	16
37	24	13	37	23	14	153422.880	11	31	18	13	31	17	14	162814.108	-11	14	2	13	14	0	14	168233.180	77
25	13	12	25	13	13	153507.511	93	31	19	13	31	18	14	163218.990	-40	10	4	7	9	4	6	168484.396	-67
25	13	12	25	12	13	153532.849	63	31	19	13	31	17	14	163236.164	-45	10	3	7	9	3	6	168485.347	85
25	14	12	25	13	13	153537.529	63	30	17	13	30	17	14	163875.094	-30	10	4	7	9	3	6	168532.664	116
25	14	12	25	12	13	153562.872	38	36	29	8	36	27	9	163880.186	213	44	31	14	44	30	15	168667.607	-75
48	36	13	48	34	14	153845.791	42	30	17	13	30	16	14	163891.711	-44	9	5	5	8	4	4	168783.533	36
24	13	12	24	12	13	153873.091	58	39	25	14	39	24	15	163932.571	19	38	24	14	38	24	15	169603.135	100
24	12	12	24	11	13	153877.030	43	30	18	13	30	17	14	163995.649	-7	43	30	14	43	29	15	169626.404	133
24	13	12	24	11	13	153900.867	35	30	18	13	30	16	14	164012.267	-20	11	7	5	10	7	4	218329.040	164
44	32	13	44	30	14	153921.625	209	29	16	13	29	16	14	164594.031	-29	13	6	8	12	6	7	230904.208	29
23	11	12	23	11	13	154148.776	88	29	17	13	29	16	14	164606.238	23	13	5	8	12	5	7	230905.554	61
23	12	12	23	10	13	154208.059	-52	29	16	13	29	15	14	164612.596	-51	11	10	2	10	10	1	231366.035	36
34	32	2	34	31	3	154280.051	-15 #	29	17	13	29	15	14	164624.783	-17	41	22	19	41	22	20	232393.578	108
22	10	12	22	10	13	154416.365	53	24	20	4	24	18	7	165059.395	81	41	22	19	41	21	20	232410.332	76 *d*
22	11	12	22	10	13	154446.726	-26	28	15	13	28	15	14	165128.605	11	11	10	1	10	10	0	232544.068	23
22	10	12	22	9	13	154448.643	55	28	15	13	28	14	14	165148.735	-13	11	9	3	10	9	2	232551.552	109
22	11	12	22	9	13	154479.067	38	28	16	13	28	15	14	165156.706	-8	40	21	19	40	20	20	233156.845	144
40	35	5	40	34	6	154483.318	151	28	16	13	28	14	14	165176.831	-37	40	22	19	40	21	20	233157.509	-45
40	35	6	40	34	7	154522.994	-77	27	14	13	27	14	14	165594.540	13	40	22	19	40	20	20	233172.480	16
21	9	12	21	9	13	154651.513	70	27	15	13	27	14	14	165613.781	2	40	33	8	40	31	9	233234.441	-45
21	10	12	21	9	13	154684.634	46	27	14	13	27	13	14	165616.684	-18	39	19	21	39	20	20	233885.703	-90
21	10	12	21	8	13	154719.195	64	27	15	13	27	13	14	165635.930	-24	39	19	21	39	19	20	233898.792	-255
45	32	14	45	31	15	154767.464	76	50	37	14	50	35	15	165637.898	-80	39	20	19	39	20	20	233899.831	-272
20	8	12	20	8	13	154857.799	133	43	29	14	43	28	15	165718.537	7	39	20	19	39	19	20	233913.309	-49
20	8	12	20	7	13	154894.501	50	26	13	13	26	13	14	165991.581	28	38	19	19	38	19	20	234626.695	314
20	9	12	20	7	13	154929.700	-7	26	13	13	26	12	14	166015.763	-30 *d*	38	19	19	38	18	20	234637.904	-19
19	7	12	19	7	13	155037.059	56	25	12	13	25	12	14	166339.303	35	38	20	19	38	19	20	234639.322	115
19	8	12	19	7	13	155074.524	33	25	13	13	25	12	14	166364.633	-2	38	20	19	38	18	20	234650.580	-169
19	7	12	19	6	13	155076.023	48	25	12	13	25	11	14	166365.795	-52	37	18	19	37	18	20	235363.284	77

TABLE 2—*Continued*

J'	K'_a	K'_c	J''	K''_a	K''_c	ν(MHz)	$o-c^a$		J'	K'_a	K'_c	J''	K''_a	K''_c	ν(MHz)	$o-c^a$		J'	K'_a	K'_c	J''	K''_a	K''_c	ν(MHz)	$o-c^a$	
37	18	19	37	17	20	235372.974	-87		17	6	12	16	6	11	280760.359	64		27	2	26	27	1	27	329974.422	24	
37	19	19	37	18	20	235374.699	80		20	2	18	19	3	17	280767.710	-179		27	1	26	27	0	27	329977.251	-93	
37	19	19	37	17	20	235384.739	265		16	6	10	15	6	9	280792.041	-211	*d*	13	12	1	12	11	2	330478.555	-78	
11	7	4	10	7	3	235713.924	-247		17	6	12	16	5	11	280802.299	-212		20	6	14	19	7	13	330620.661	52	
36	17	19	36	17	20	236094.531	88		18	5	14	17	4	13	280806.970	-217		19	7	12	18	8	11	330644.446	-1	
36	17	19	36	16	20	236102.874	71		19	4	16	18	3	15	280827.856	-242		20	6	14	19	6	13	330659.421	-159	
36	18	19	36	17	20	236104.800	107		20	3	18	19	2	17	280859.061	-269		21	5	16	20	5	15	330674.672	38	*d*
36	18	19	36	16	20	236113.178	125		21	2	20	20	1	19	280912.437	-104		26	0	26	25	1	25	330688.471	-19	
23	5	19	23	4	20	242598.845	162		15	8	8	14	8	7	280935.424	64		19	8	12	18	7	11	330720.245	43	
23	4	19	23	3	20	242600.639	78		15	7	8	14	7	7	280943.463	29		22	4	18	21	4	17	330723.586	55	*d*
9	7	2	8	5	3	245085.317	28		15	8	8	14	7	7	280984.650	-171		26	0	26	25	0	25	330738.888	67	*d*
12	7	5	11	7	4	245525.327	195		18	5	13	17	6	12	293189.487	-108		18	8	10	17	9	9	330741.798	69	
11	8	3	10	8	2	245598.337	200		19	4	15	18	5	14	293201.607	-113		25	1	24	24	2	23	330745.281	7	
9	8	1	8	6	2	246293.459	54		17	6	11	16	7	10	293210.326	-76		26	1	26	25	0	25	330789.203	52	
16	4	12	15	5	11	255766.615	275		20	3	17	19	4	16	293226.249	-80		25	2	24	24	1	23	330840.737	-52	
17	3	14	16	4	13	255777.048	218		17	6	11	16	6	10	293251.131	45	*d*	16	11	6	15	11	5	330872.528	-40	
14	6	8	13	6	7	255907.119	30		20	3	17	19	3	16	293269.997	-76	*d*	17	10	8	16	10	7	331095.342	-26	
14	7	8	13	7	7	255908.950	13		18	6	13	17	5	12	293272.285	-45		16	10	6	15	10	5	334296.573	-11	
10	10	1	9	9	0	257119.076	77		19	5	15	18	4	14	293286.484	-52		13	13	1	12	12	0	335239.702	113	
10	10	0	9	9	1	257383.318	-76		16	7	9	15	8	8	293304.954	-14		13	13	0	12	12	1	335275.248	19	
13	9	5	12	9	4	267666.295	-148		16	8	9	15	7	8	293386.168	-2		16	15	2	15	15	1	335349.461	30	
44	22	22	44	21	23	267739.447	-73		22	1	21	21	2	20	293461.339	-103		16	15	1	15	15	0	335412.308	45	
44	23	22	44	22	23	267741.817	-279		23	0	23	22	1	22	293504.294	-92		15	11	4	14	11	3	335995.848	-11	
44	23	22	44	21	23	267762.328	-78		22	2	21	21	2	20	293507.894	-18		48	21	27	48	20	28	336893.455	-157	
9	7	3	8	5	4	268119.889	-12		22	1	21	21	1	20	293508.667	-240		48	22	27	48	21	28	336894.278	-125	
12	9	3	11	9	2	268174.499	-65		23	0	23	22	0	22	293554.562	121	*d*	48	22	27	48	20	28	336908.365	-146	
17	4	13	16	5	12	268241.939	117		23	1	23	22	0	22	293604.549	51		47	20	27	47	20	28	337338.878	-153	
16	5	11	15	6	10	268246.709	181		23	1	22	22	1	21	304579.873	-153	*d*	47	20	27	47	19	28	337352.833	-132	
18	3	15	17	4	14	268257.283	-38		23	2	22	22	1	21	304626.714	-135		47	21	27	47	20	28	337353.723	-6	
19	2	17	18	3	16	268279.671	15		19	5	14	18	6	13	305669.117	236		47	21	27	47	19	28	337367.658	-6	
18	3	15	17	3	14	268302.038	195	*d*	20	4	16	19	5	15	305685.965	226		46	19	27	46	19	28	337774.208	-37	
20	1	19	19	2	18	268308.416	203		18	6	12	17	6	11	305717.287	53	*d*	46	19	27	46	18	28	337788.329	173	
16	6	11	15	5	10	268331.554	112		21	3	18	20	4	17	305722.014	116		46	20	27	46	19	28	337788.845	-11	
15	6	9	14	6	8	268342.794	188	*d*	20	4	16	19	4	15	305727.798	151	*d*	46	20	27	46	18	28	337802.974	208	
18	4	15	17	3	14	268346.596	231		17	7	10	16	8	9	305737.628	-1		45	18	27	45	18	28	338186.269	132	
20	2	19	19	1	18	268404.197	288		19	6	14	18	5	13	305750.296	-182		45	18	27	45	17	28	338200.625	110	*d*
14	7	7	13	7	6	268611.533	-38		18	7	12	17	6	11	305757.374	200		45	19	27	45	17	28	338215.041	147	
10	8	2	9	6	3	269555.960	156		24	0	24	23	1	23	305763.436	51		44	17	27	44	17	28	338575.393	-238	
41	19	22	41	19	23	269821.478	44		20	5	16	19	4	15	305769.670	114		44	17	27	44	16	28	338590.185	-159	*d*
41	19	22	41	18	23	269842.764	84		21	4	18	20	3	17	305808.580	66		16	14	3	15	14	2	338933.399	182	
41	20	22	41	19	23	269845.280	18		12	10	2	11	9	3	307513.687	-87		43	16	27	43	15	28	338958.959	62	*d*
41	20	22	41	18	23	269866.412	-95		15	9	6	14	9	5	307974.876	149		43	17	27	43	15	28	338974.280	90	
24	3	21	24	3	22	270456.997	-90		11	10	1	10	8	2	308178.814	142		42	15	27	42	15	28	339290.841	-53	
40	18	22	40	18	23	270462.401	36		15	10	6	14	9	5	308429.039	133		42	15	27	42	14	28	339307.017	-15	*d*
40	18	22	40	17	23	270484.173	-9		26	1	25	26	1	26	317468.413	30		42	16	27	42	14	28	339323.137	-31	
40	19	22	40	18	23	270486.690	-41		26	2	25	26	1	26	317515.866	-36		16	12	5	15	12	4	339478.251	69	
24	4	21	24	3	22	270495.021	-248		26	1	25	26	0	26	317518.737	23		41	14	27	41	14	28	339618.125	-175	
24	3	21	24	2	22	270502.032	-36		20	5	15	19	5	14	318189.038	-91	*d*	41	14	27	41	13	28	339635.341	-211	*d*
40	19	22	40	17	23	270508.408	-141		21	4	17	20	4	16	318217.873	-193	*d*	41	15	27	41	13	28	339652.498	-306	
24	4	21	24	2	22	270540.234	-16		18	7	11	17	7	10	318223.477	-13	*d*	40	13	27	40	13	28	339926.528	-63	
25	5	21	25	4	22	271952.440	98		20	6	15	19	5	14	318229.305	-28		40	13	27	40	12	28	339945.206	-15	*d*
25	4	21	25	3	22	271961.660	-165		22	4	19	21	3	18	318326.867	54		40	14	27	40	12	28	339963.702	-148	
29	7	22	29	7	23	276381.724	-196		17	8	9	16	9	8	318336.877	144		20	7	13	19	8	12	343097.903	18	
29	7	22	29	6	23	276418.290	-229	*d*	17	8	9	16	8	8	318372.294	-46		21	6	15	20	7	14	343100.119	-18	
29	8	22	29	6	23	276455.030	-88		17	9	9	16	9	8	318374.143	-9		22	5	17	21	6	16	343132.101	79	
22	0	22	21	1	21	280349.034	-167		23	3	21	22	3	20	318709.052	48		20	7	13	19	7	12	343135.096	76	*d*
22	0	22	21	0	21	280398.913	-89	*d*	23	2	21	22	2	20	318711.065	5		21	6	15	20	6	14	343138.055	-8	*d*
22	1	22	21	0	21	280448.663	-139		32	7	26	32	6	27	329155.173	0		27	0	27	26	1	26	343159.496	5	
17	5	12	16	6	11	280718.450	-200		32	6	26	32	5	27	329157.289	122		26	1	25	25	2	24	343165.206	65	
18	4	14	17	5	13	280721.168	-238		31	5	26	31	5	27	329311.849	95		21	7	15	20	6	14	343176.043	55	
19	3	16	18	4	15	280739.572	-242		31	6	26	31	5	27	329348.145	155		19	9	11	18	9	10	343208.255	-154	
16	6	10	15	7	9	280750.745	-198		15	12	3	14	12	2	329887.623	-29		23	4	19	22	5	18	343228.094	128	
19	9	11	18	8	10	343245.887	33		18	9	9	17	9	8	343435.909	49		24	4	21	23	4	20	344044.294	4	
23	5	19	22	4	18	343308.070	-37		24	3	21	23	4	20	344006.246	138		24	3	21	23	3	20	344047.399	-251	

TABLE 2—*Continued*

J' K'_a K'_c	J'' K''_a K''_c	ν(MHz)	$o-c$[a]	J' K'_a K'_c	J'' K''_a K''_c	ν(MHz)	$o-c$[a]	J' K'_a K'_c	J'' K''_a K''_c	ν(MHz)	$o-c$[a]
24 4 21	23 3 20	344085.867	34	39 11 28	39 11 29	353002.971	219	12 12 1	11 10 2	361193.636	150
25 3 23	24 2 22	344137.378	53	39 12 28	39 11 29	353023.433	64	50 21 29	50 20 30	362270.109	125 *d*
17 10 7	16 10 6	344632.608	127	39 11 28	39 10 29	353024.999	513	17 13 5	16 13 4	362566.847	-221
13 10 3	12 9 4	345329.521	-33	39 12 28	39 10 29	353045.147	44	17 12 6	16 11 5	362842.783	-284
14 12 3	13 11 2	346283.588	121	38 11 28	38 10 29	353267.699	-114	17 14 4	16 14 3	363053.430	36
12 10 3	11 8 4	346588.909	188	38 10 28	38 9 29	353269.137	-46	48 19 29	48 18 30	363060.245	-6 *d*
12 8 4	11 6 5	348205.230	-23	12 9 4	11 7 5	353410.363	-20	47 18 29	47 17 30	363426.002	68 *d*
51 23 28	51 23 29	348683.973	194	21 7 14	20 8 13	355578.133	12	47 19 29	47 17 30	363439.013	14
51 23 28	51 22 29	348698.739	223 *d*	22 6 16	21 7 15	355588.946	-16	46 17 29	46 16 30	363773.261	214 *d*
51 24 28	51 22 29	348713.454	199	21 7 14	20 7 13	355614.438	-71 *d*	42 13 29	42 13 30	364973.515	183
50 22 28	50 21 29	349174.313	-189 *d*	22 6 16	21 6 15	355626.121	-32 *d*	42 13 29	42 12 30	364990.230	126 *d*
16 13 3	15 13 2	349204.297	23	28 0 28	27 1 27	355630.710	-80	42 14 29	42 12 30	365006.864	-14
12 11 2	11 9 3	349999.014	-73	20 8 12	19 8 11	355658.514	187 *d*	40 12 29	40 11 30	365504.102	-182
48 20 28	48 20 29	350041.463	-17	22 7 16	21 6 15	355663.390	47	40 11 29	40 10 30	365505.218	-281
48 20 28	48 19 29	350055.103	-143 *d*	20 9 12	19 8 11	355693.994	-20	12 8 5	11 6 6	365698.629	-105
48 21 28	48 19 29	350068.967	-43	27 2 26	26 1 25	355715.873	24	39 11 29	39 10 30	365740.211	16
13 10 3	12 8 4	350766.812	298	23 6 18	22 5 17	355728.614	69	39 10 29	39 9 30	365741.862	195
44 16 28	44 16 29	351544.653	-154	28 1 28	27 0 27	355731.570	80	38 10 29	38 9 30	365962.512	-93
43 15 28	43 15 29	351871.311	-84	26 2 24	25 3 23	355747.174	-107	38 9 29	38 8 30	365964.397	74
43 15 28	43 14 29	351886.504	-86 *d*	26 3 24	25 2 23	355837.689	-82	37 8 29	37 8 30	366145.666	14
25 3 22	24 4 21	352026.753	-11	24 4 20	23 5 19	355909.861	11	37 9 29	37 8 30	366171.906	-135
16 11 5	15 11 4	352056.525	-206	24 5 20	23 4 19	355987.653	-136	37 8 29	37 7 30	366173.813	-178
25 3 22	24 3 21	352064.696	-250	14 13 1	13 12 2	356261.432	83	31 3 29	31 2 30	367183.671	66
25 4 22	24 4 21	352069.646	-159	18 11 8	17 10 7	356362.947	105	31 2 29	31 1 30	367186.676	-73
25 4 22	24 3 21	352107.915	-72	16 12 4	15 12 3	358470.933	8	19 10 9	18 11 8	368505.768	-76
42 14 28	42 14 29	352179.492	-293	16 12 5	15 11 4	359396.933	-258	19 10 9	18 10 8	368521.254	-73
13 11 2	12 9 3	352321.844	32	17 15 3	16 15 2	359710.618	-175	19 11 9	18 11 8	368536.810	-107
41 13 28	41 13 29	352470.822	134	17 15 2	16 15 1	360338.759	110	19 11 9	18 10 8	368552.250	-151
40 13 28	40 12 29	352763.678	27	17 11 6	16 11 5	361053.983	189	18 12 7	17 12 6	368969.658	-57
40 12 28	40 11 29	352764.534	27	14 14 1	13 13 0	361164.478	170	24 19 6	23 19 5	517034.426	-127
40 13 28	40 11 29	352783.442	72	14 14 0	13 13 1	361182.263	105	23 17 6	22 17 5	517179.548	-327

TABLE 3

Newly Observed Millimeter-/Submillimeter-Wave Transitions between the $\nu_5 = 1$ and $\nu_9 = 2$ Vibrational States

J' K'_a K'_c	J'' K''_a K''_c	ν(MHz)	$o-c$[a]	J' K'_a K'_c	J'' K''_a K''_c	ν(MHz)	$o-c$[a]
$\nu_5 \leftarrow 2\nu_9$				$2\nu_9 \leftarrow \nu_5$			
29 22 8	29 16 13	118480.492	-10	39 27 12	39 32 7	131249.217	-108
40 30 10	40 26 15	151699.241	-2	39 28 11	39 32 8	139031.550	-28
33 24 9	33 20 14	151862.154	27	35 24 12	35 27 9	139610.536	-105
32 23 9	32 19 14	166405.081	66	31 20 12	31 22 9	141897.855	-62
32 23 9	32 18 14	166417.012	117	40 27 13	40 30 10	165700.627	90
37 29 9	37 23 14	166774.110	-29	25 2 23	24 4 20	332162.857	-56
36 28 9	36 22 14	167221.795	-152	25 3 23	24 5 20	332179.977	-73
32 14 19	32 10 22	255763.871	267	25 3 23	24 4 20	332208.441	97
24 4 20	23 3 21	340356.928	63	24 2 22	23 4 19	346127.517	144
24 5 20	23 3 21	340385.200	41	24 3 22	23 5 19	346141.426	130
24 4 20	23 2 21	340399.321	-97				
24 5 20	23 2 21	340427.742	29				
24 3 21	23 2 22	352182.610	-240				
25 5 20	24 4 21	366575.364	148				
25 6 20	24 4 21	366601.472	28				
25 5 20	24 3 21	366613.424	26				
25 6 20	24 3 21	366639.684	58				

[a] Observed − calculated ($o - c$) are given in kHz. All experimental uncertainties are 100 kHz.

TABLE 4
Spectroscopic Parameters (in MHz) for the ν_5 and $2\nu_9$ Vibrational States of HNO_3[a]

Parameter	Artificial Splitting Analysis		Induced Splitting Analysis	
	ν_5	$2\nu_9$	ν_5	$2\nu_9$
ν_0	26355017.84[b]	26874843.54(16)	26568683.31[b]	26661177.91(16)
A	12962.3000(328)	12962.6504(231)	12958.6045(678)	12966.4697(654)
B	12085.74056(3289)	12025.8774(232)	12140.5660(663)	11970.9309(638)
C	6242.05889(34)	6242.23697(35)	6234.3657(595)	6249.9286(595)
D_{ab}	-196.1026(734)	-184.5912(587)	-209.4372(644)	-170.9494(741)
D_{abJ} $\cdot 10^3$	2.48709(3427)	1.5035(656)	2.2231(559)	1.5521(603)
D_{abK} $\cdot 10^3$	-2.3144(145)	–2.0246(305)	-1.6356(590)	-1.0584(1006)
D_{abJJ} $\cdot 10^8$	-9.372(491)	–	-2.070(143)	1.366(369)
D_{abJK} $\cdot 10^7$	–	–2.927(94)	–	-1.385(142)
D_{abKK} $\cdot 10^8$	-6.66(27)	–	–	11.93(46)
Δ_J $\cdot 10^3$	9.792336(18338)	8.434742(22236)	9.11824(1334)	9.03203(1086)
Δ_{JK} $\cdot 10^3$	-7.75775(6226)	-3.29078(6177)	-5.26789(6203)	-4.29228(6810)
Δ_K $\cdot 10^3$	8.83441(4213)	5.80608(3323)	6.74679(10154)	5.79835(9758)
δ_J $\cdot 10^3$	4.179128(9149)	3.59440(1101)	3.89825(670)	3.83703(532)
δ_K $\cdot 10^3$	8.93080(1936)	6.30322(1210)	8.47317(3010)	7.38143(2918)
H_J $\cdot 10^9$	7.424(945)	–	–	-9.393(827)
H_{JK} $\cdot 10^7$	–	2.0485(518)	1.1842(505)	0.9881(1004)
H_{KJ} $\cdot 10^7$	–	-3.1527(902)	-3.4765(939)	-1.8510(1702)
H_K $\cdot 10^8$	–4.568(368)	–	24.587(293)	10.04(90)
h_J $\cdot 10^9$	4.415(468)	–	–	-3.965(412)
h_{JK} $\cdot 10^8$	–8.082(207)	14.00(35)	1.04(29)	3.216(344)
h_K $\cdot 10^7$	1.638(13)	0.7772(208)	0.9558(323)	–
Fourier Expansion of Rotational Constants				
ρ (dimensionless)	0.978793	0.978793	–	0.978793
E_ρ	-17.71(1)	-25.40(1)	–	-43.15(1)
$E_{\rho J}$ $\cdot 10^4$	-4.22(15)	-12.8(2)	–	-15.7(3)
$E_{\rho K}$ $\cdot 10^3$	–	2.60(6)	–	3.06(7)
$E_{\rho\pm}$ $\cdot 10^4$	3.92(9)	3.58(9)	–	6.99(25)
$E_{\rho Dab}$ $\cdot 10^4$	-2.0(2)	–	–	-1.6(3)
$E_{\rho JJ}$ $\cdot 10^7$	–	–	–	-1.6(2)
$E_{\rho\pm J}$ $\cdot 10^8$	–	–	–	8.8(22)
Interaction Constants				
C_{ab}	-18.2382(465)		2.4633(275)	
C_{abJ} $\cdot 10^7$	–		-1.246(79)	
F_0	–		255765.17(6)	
F_J	37.57560(7035)		-8.214497(12382)	
F_K	-45.0138(813)		7.71582(2166)	
F_{JJ} $\cdot 10^4$	3.1224(1178)		1.0857(893)	
F_{JK} $\cdot 10^4$	-9.2498(2223)		-1.0585(1038)	
$F_\pm$	19.90903(3753)		-3.44922(246)	
$F_{\pm J}$ $\cdot 10^5$	1.882(376)		6.1689(5187)	
$F_{\pm K}$ $\cdot 10^4$	-3.0170(651)		2.7490(625)	
$F_{\pm JK}$ $\cdot 10^8$	2.686(83)		–	
$F_{\pm JKK}$ $\cdot 10^8$	-3.079(104)		–	
Fourier Expansion of Interaction Constants				
$F_{\rho 0}$	21.67(4)		–	
$F_{\rho\pm}$ $\cdot 10^4$	-9.74(19)		–	

[a] Estimated errors in parenthesis represent one standard deviation. Enough digits are supplied to reproduce the spectra.
[b] The band center was fixed at the value determined from the infrared/microwave analysis in Ref. (*8*).

TABLE 5
Comparison of Spectroscopic Parameters (in MHz)

Parameter	Artificial Splitting Analysis	Induced Splitting Analysis
Average values		
A	12962.4752(201)[a]	12962.5371(471)
B	12055.8090(232)	12055.7485(460)
C	6242.14793(35)	6242.1471(421)
D_{ab}	-190.3469(470)	-190.1933(491)
Torsional splitting		
E_ρ	-43.11(1)[b]	-43.15(1)
Difference in perturbed band centers		
$\Delta E = E_{2\nu9}-E_{\nu5}$	519825.700(160)	519825.497(160)

[a] Estimated errors in parenthesis represent one standard deviation.
[b] Represents the combined torsional splitting, $E_{\rho,\nu5} + E_{\rho,2\nu9}$.

Both analyses accurately predict the observed 1.4 intensity ratio of the two infrared bands (*5*). For the induced splitting analysis, the ratio of the mixing coefficients of the $J = 0$ levels predict an intensity ratio of 1.43, while ratio of the torsional splitting parameters, E_ρ^ν in Eq. [3], predicts an intensity ratio of 1.37.

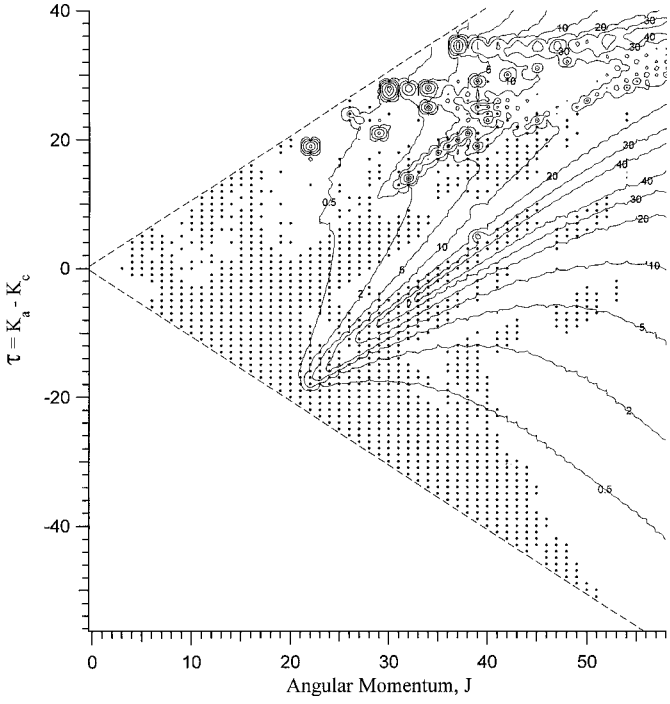

FIG. 1. Solid circles (●) show the locations of the rotational levels included in the fit of the ν_5 microwave transitions. An overlapping contour plot of the mixing coefficients from the artificial splitting analysis illustrates the location of the perturbations with $2\nu_9$. The number on the contour represents the percentage of the total wave function belonging to $2\nu_9$. In the induced spitting analysis, the mixing starts at 41% with the $J = 0$ rotational states. The analysis and data for $2\nu_9$ results in a similar plot.

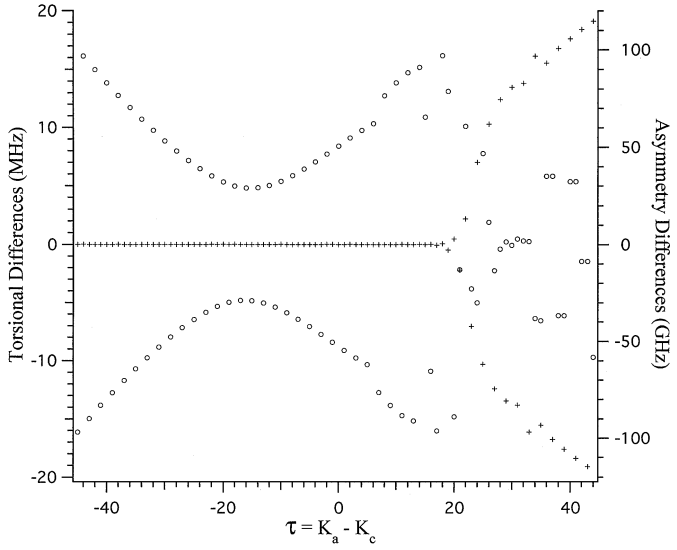

FIG. 2. Rotational dependence of the torsional splitting for $J = 45$ in ν_5 calculated from the artificial splitting analysis. The differences between the K_a, K_c and $K_a + 1$, K_c energy levels are shown on two different scales; the left axis shows the torsional contribution, indicated by open circles (○), and the right axis shows the asymmetry splitting contribution, indicated by plus signs (+). The torsional dependence is easily recognized in the symmetric top limit. When the asymmetry splitting becomes comparable to the torsional splitting, rotational energy level labeling becomes ambiguous and no systematic pattern is discernable. Far into the asymmetric limit, a pattern reemerges when the energy levels with K_a, K_c and K_a, $K_c + 1$ become clustered (8).

The $\nu_5/2\nu_9$ band of HNO_3 is a particularly stringent test for the capacity of microwave analyses to synthesize infrared spectra because of the strong perturbations between the two states and the extensive, high quality infrared data that sets the standard for comparison. Figure 3 shows the locations of the experimentally determined $\nu_5 = 1$ infrared energy levels of Refs. (*5*). The accuracy of the *predictions* of these same levels from the results of the microwave analysis and the infrared analysis of Ref. (*5*) are also indicated by symbols on the graph and summarized in Table 6. Inspection of Table 6 shows that the distribution of errors for the microwave predictions of the infrared energy levels and the predictions of these same levels using the spectroscopic parameters from Ref. (*5*) are about the same, thus showing the synthesis capability of the microwave analysis for this complex dyad. However, the synthesis is in all likelihood much better. For many of the infrared levels the corresponding pure rotational spectrum has been directly measured to microwave accuracy ($\sim$0.1 MHz) and that part of the synthesized spectrum should be more accurate by approximately the ratios of the measurement uncertainties ($\sim \times 100$).

Inspection of Fig. 3 shows that the distribution of error in $J, \tau = K_a - K_c$ for ν_5 is similar between the infrared analysis and the microwave predictions of the infrared levels, with most of the error located at the very edge of the infrared data set. A similar distribution of error is observed for $2\nu_9$. From the available information, it is not possible to tell if this is because

TABLE 6
Distribution of Error in the Predictions of the Infrared Energy Levels from the Results of the Microwave and Infrared Analyses[a]

Number of IR energy levels	ν_5 1207		$2\nu_9$ 1113		combined 2320	
Analysis	Micro-wave	Infrared[b]	Micro-wave	Infrared[a]	Micro-wave	Infrared[a]
Percentage of levels between (cm^{-1})						
$0 \le \lvert Obs\text{-}Calc \rvert < 0.001$	94.95	92.96	96.68	94.25	95.78	93.58
$0.001 \le \lvert Obs\text{-}Calc \rvert < 0.002$	3.40	6.55	2.96	5.66	3.19	6.12
$0.002 \le \lvert Obs\text{-}Calc \rvert < 0.004$	1.41	0.50	0.36	0.09	0.91	0.30
$\lvert Obs\text{-}Calc \rvert \ge 0.004$	0.25	0.00	0.00	0.00	0.13	0.00

[a] The experimental infrared energy levels, along with the spectroscopic parameters used to generate the infrared predictions, were reported in Ref. (*5*).

the microwave model extrapolations deteriorate very rapidly at the edge of the infrared data set, or if the infrared measurements which led to these levels are of lesser accuracy than the rest of the infrared data.

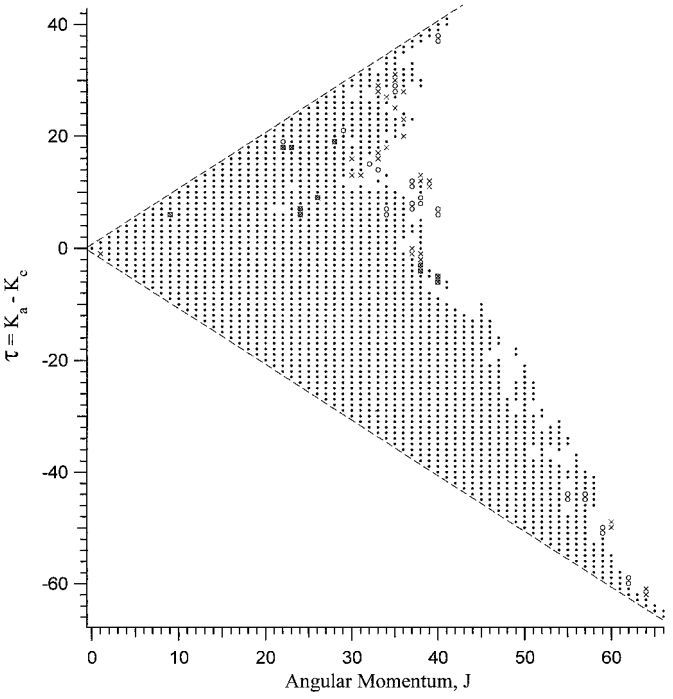

FIG. 3. The plot shows the locations of the experimentally determined infrared energy levels from Refs. (*5*) used to test the predictions of the microwave and infrared analyses. The spectroscopic parameters of Ref. (*5*) were used to generate the infrared predictions. The rms deviation of that analysis, $\sigma_{rms} = 0.51 \times 10^{-3}$ cm^{-1}, was used as a benchmark to test the microwave predictions. The solid circles (●) indicate levels with (obs − calc) $< 3\sigma_{rms}$ for both the infrared and microwave predictions. Levels with a cross sign (×) indicate microwave predictions with (obs − calc) $> 3\sigma_{rms}$ and levels with an open circle (○) indicate infrared predictions with (obs − calc) $> 3\sigma_{rms}$.

V. CONCLUSIONS

In this paper, we have shown by analysis of the pure rotational spectrum of both the ground and $\nu_5/2\nu_9$ dyad of HNO_3 that it is possible to synthesize to high accuracy the rotational manifold of the corresponding infrared band. This case is particularly challenging because of the complex torsional structure and strong mixing of the two states. Additionally, the quality of the infrared analysis sets a high standard for comparison. We conclude that this approach should be especially advantageous for heavier species, whose Doppler-limited infrared spectrum is too crowded for a detailed analysis.

ACKNOWLEDGMENTS

We thank Agnes Perrin for providing us with the details of the infrared analysis. D.T.P. thanks the NASA–ASEE Summer Faculty Program and John C. Pearson for sponsoring his visit to the Jet Propulsion Laboratory. We also acknowledge NASA for its support of this work.

REFERENCES

1. P. Brockman, C. H. Bair, and F. Allario, *Appl. Opt.* **17,** 91–100 (1978).
2. A. G. Maki and J. S. Wells, *J. Mol. Spectrosc.* **108,** 17–30 (1984).
3. T. Giesen, M. Harter, R. Schieder, G. Winnewisser, and K. M. T. Yamada, Z. *Naturforsch. A* **43,** 402–406 (1988).
4. A. G. Maki and J. S. Wells, *J. Mol. Spectrosc.* **152,** 69–79 (1992).
5. A. Perrin, V. Jaquen, A. Valentin, J.-M. Flaud, and C. Camy-Peyret, *J. Mol. Spectrosc.* **157,** 112–121 (1993), doi:10.1006/jmsp.1993.1009.
6. R. L. Crownover, R. A. Booker, F. C. De Lucia, and P. Helminger, *J. Quant. Spectrosc. Radiat. Transfer* **40,** 39–46 (1988).
7. T. M. Goyette, C. D. Paulse, L. C. Oesterling, and F. C. De Lucia, *J. Mol. Spectrosc.* **167,** 365–374 (1994), doi:10.1006/jmsp.1994.1242.
8. L. H. Coudert and A. Perrin, *J. Mol. Spectrosc.* **172,** 352–368 (1995), doi:10.1006/jmsp.1995.1184.
9. T. M. Goyette, L. C. Oesterling, D. T. Petkie, R. A. Booker, P. Helminger, and F. C. De Lucia, *J. Mol. Spectrosc.* **175,** 395–410 (1996), doi:10.1006/jmsp.1996.0046.

10. D. T. Petkie, T. M. Goyette, R. P. A. Bettens, S. P. Belov, S. Albert, P. Helminger, and F. C. De Lucia, *Rev. Sci. Instrum* **68,** 1675–1683 (1997).
11. S. Albert, D. T. Petkie, R. P. A. Bettens, S. P. Belov, and F. C. De Lucia, *Anal. Chem.* **70,** 719A–727A (1998).
12. R. R. Friedl, M. Birk, J. J. Oh, and E. A. Cohen, *J. Mol. Spectrosc.* **170,** 383–396 (1995), doi:10.1006/jmsp.1995.1079.
13. H. M. Pickett, *J. Mol. Spectrosc.* **148,** 371–377 (1991).
14. H. M. Pickett, *J. Chem. Phys.* **107,** 6732–6735 (1997).
15. A. P. Cox, M. C. Ellis, C. J. Attfield, and A. C. Ferris, *J. Mol. Struct.* **320,** 91–106 (1994).
16. A. Perrin, J.-M. Flaud, C. Camy-Peyret, B. P. Winnewisser, S. Klee, A. Goldman, F. J. Murcray, R. D. Blatherwick, F. S. Bonomo, and D. G. Muircray, *J. Mol. Spectrosc.* **166,** 224–243 (1994), doi:10.1006/jmsp.1994.1187.
17. J. K. G. Watson, *in* "Vibrational Spectra and Structure" (J. R. Durig, Ed.), Vol. 6, pp. 1–89, Elsevier. Amsterdam, 1977.